Integrin Ligands with α/β-Hybrid Peptide Structure: Design, Bioactivity, and Conformational Aspects

Integrin Ligands with α/β-Hybrid Peptide Structure: Design, Bioactivity, and Conformational Aspects

Rossella De Marco,[1] Alessandra Tolomelli,[1] Eusebio Juaristi,[2] and Luca Gentilucci[1,*]

[1] *Department of Chemistry "G. Ciamician", University of Bologna, via Selmi 2, 40126-Bologna ITALY*

[2] *Department of Chemistry, Centro de Investigacion y de Estudios Avanzados del IPN, Avenida IPN # 2508, esquina Ticoman, Mexico D.F. 07360 MEXICO*

* Tel: ++39-051-209-9450; Fax: +39-051-209-9456; E-mail: luca.gentilucci@unibo.it; web: http://www.ciam.unibo.it/gentilucci

Synopsis: Integrins are cell surface receptors for proteins of the extracellular matrix and plasma-borne adhesive proteins. Their involvement in diverse pathologies prompted medicinal chemists to develop small-molecule antagonists, and very often such molecules are peptidomimetics designed on the basis of the short native ligand-integrin recognition motifs. This review deals with peptidomimetic integrin ligands composed of α- and β-amino acids. The roles exerted by the β-amino acid components are discussed in terms of biological activity, bioavailability, and selectivity. Special attention is paid to the synthetic accessibility and efficiency of conformationally constrained heterocyclic scaffolds incorporating α/β-amino acid span.

Keywords: β-amino acid; peptidomimetic; heterocycle; integrin; cancer

1. Introduction

Peptides fulfill a variety of biological and physiological functions, and for this reason natural and synthetic peptides have found a number of biomedical applications. Besides to the well-known bioactive peptides of natural origins, such as the anticancer, antibiotic, hormone, immunoactive, neuromodulator, and opioid peptides, new examples have been recently described for bio- and nanotechnological applications. Examples are peptide-derived vaccines, drug-delivery systems, radiolabeled probes, biomaterials for tissue engineering, self-assembling peptides, microchips, nanomaterials, biosensors, bioelectronic devices, and peptide-metal nanowires.[1]

Unfortunately, many potential applications of native peptides remain unpractical, due to their limited stability *in vivo*, and to their poor ability to cross biological barriers (e.g. gut, blood-brain-barrier). Furthermore, peptides are rather flexible entities, which may result in lack of receptor selectivity. Therefore, much effort has been dedicated to the design of peptidic derivatives or analogues with improved stability, biological functions, and with the appropriate spatial orientation of the pharmacophoric groups. Among diverse strategies, the introduction of non-proteogenic amino acid residues is an effective and by now well-established method for the preparation of suitable peptidomimetics, i.e. compounds whose essential pharmacophore elements mimic natural peptides in 3D space, and which retain the ability to interact with the biological

targets.[2,3] In this regard, within the many potential non-proteogenic amino acid residues to be used, the β-amino acids[4] have gained special attention.[5] Indeed, there exists a significant number of naturally occurring β-amino acids found in several natural products, for instance in fungal peptide antibiotics.[3,6] β-Amino acids can be classified as β^3, when the side chain is located adjacent to the β-amino group, or β^2, when the side chain is adjacent to the carboxylic acid group (Figure 1). β^2-Amino acids are generally less synthetically accessible relative to their β^3-counterparts.[6] From a conformational point of view, according to the convention of Banerjee and Balaram,[7] the torsional degrees of freedom in a β-amino acid are defined as ϕ (N-Cβ), θ (Cβ-Cα), and ψ (Cα-C=O), respectively (Figure 1).

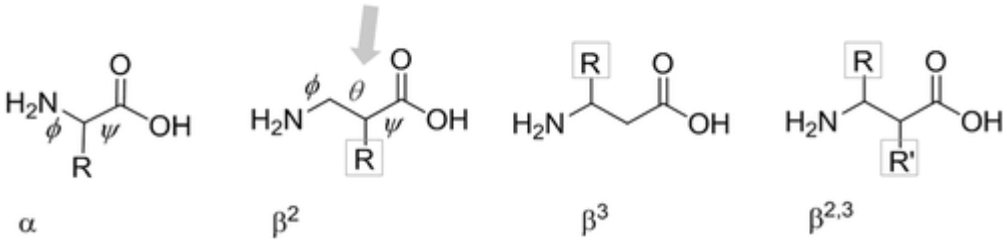

Figure 1 -Structures of *α*-, *β*2-, *β*3-, and *β*2,3-amino acids (following Seebach's nomenclature[6]); the gray arrow shows the extra torsional angle θ (convention of Banerjee and Balaram[7]).

In spite of the extra C-C bond compared to α-amino acid residues, β-amino acids can afford well-defined secondary structures in β-peptides.[8] Indeed, oligomers composed of all β-amino acids, or hybrid α/β-peptides[9,10] have been extensively investigated for their tendency to adopt well-defined secondary structures,[11] in particular various types of helices.[12] Cyclic β-amino acids can further restrain peptide conformations as the C2-C3 bond becomes part of a ring.[13,14] Folding oligomeric peptidomimetics are often referred to as "foldamers".[15,16]

In this review, we focus on the use of β-amino acids and β-amino acid-derived scaffolds for the preparation of small-molecule integrin ligands with α/β-hybrid peptidic structure. Our aim is not to include all the available literature on the topic,[5,6,10] but rather to discuss with the aid of specific examples the impact that β-amino acid residues have on biological activity, peptide stability, selectivity, and finally on three-dimensional (3D) structures. In particular, special attention is dedicated to the synthesis and use of heterocyclic scaffolds derived from β-amino acids. Very often, the preparation of scaffold-containing peptidomimetics requires multistep

strategies, resulting in very low yields. Besides, many synthetic methodologies are not flexible and cannot provide structural and functional diversity in the target integrin ligands.

Furthermore, the conformational analysis of the β-amino acid peptidomimetics of interest appears to be fundamental for the comprehension of the chemistry and pharmacology of small-molecule integrin ligands. As a consequence, a central goal in this review is to show how the development of synthetic protocols for the preparation of conformationally constrained peptidic derivatives that maintain the required 3D disposition of the essential pharmacophores is currently of utmost relevance.

2. Integrins and their ligands

Integrins are heterodimeric, non-covalently bound proteins expressed on cell surfaces that mediate cell-cell and cell-matrix adhesion. These receptors constitute a family of 24 combinations of diverse α- and β-chains. Integrins regulate several aspects of cell behavior, such as cell proliferation, death, differentiation, and migration,[17,18] so they may represent privileged targets for therapeutic interventions.[19,20] For instance, αvβ3 integrin is responsible for cell adhesion to proteins of the extracellular matrix (ECM), a process involved in the construction of new blood vessels (angiogenesis). By contrast, the αIIbβ3 (or GPIIb/IIIa) integrin plays a fundamental role in the aggregation of platelets mediated by fibrinogen. On the other hand, integrin α4β7 is critical in lymphocyte adhesion to the gut. Integrin α4β1 (VLA-4, very late activating antigen-4) is involved in cancer, diabetes and inflammatory diseases such as rheumatoid arthritis. It is responsible for the recruitment of leukocytes into inflamed tissues, and in the migration of activated lymphocytes during the immune response. In general, each of the 24 integrins has a specific function; however, a certain functional redundancy exists among integrins in some processes. For instance, the integrins α2β1, α3β1, α9β1, αvβ5, αvβ6, α5β1, are all up-regulated during wound healing. Beside, while some extracellular ligands are recognized by a specific integrin, other ligands show promiscuous interactions with diverse integrins; an example is represented by collagen, which can bind all integrins α1β1, α2β1, α10β1, and α11β1, albeit with different affinity.

The involvement of integrins in important pathologic processes inducted many research groups to block their functioning by means of monoclonal antibodies,[19] or small-molecule antagonists of peptidic[20,21] and non-peptidic structure.[22,23,24] More recently, the new possibilities offered by nanotechnology led to the design of molecular devices functionalized with integrin ligands, to provide nanotools for integrin-mediated drug delivery,[25,26] imaging,[27] or for theranostic applications.[28,29,30]

The aim to develop specific integrin antagonists with appropriate pharmaceutical properties has been challenging. Many of the integrin superfamily members, including αIIbβ3, αvβ3, α5β1, αvβ1, recognize the Asp-Gly-Arg (RGD) tripeptidic sequence (Figure 2A), an epitope shared by several proteins of the ECM including vitronectin (VN), fibronectin (FN), fibrinogen (FB), osteopontin, and bone sialoprotein.[19] Other integrins interact with their ligands by adhesion to somewhat different recognition motifs. For instance, both α4 integrins (α4β1 and α4β7) recognize a Leu-Asp-Val-Pro (LDVP) motif (Figure 2A) in the spliced CS-1 region in plasma FN, and a Leu-Asp-Thr-Ser (LDTS) sequence in the mucosal addressin cell adhesion molecule-1 (MAdCAM-1).[19,31]

Recently, the use of antagonist molecules capable to target two or more integrins (in particular the RGD-binding ones) has been proposed.[32] Indeed, it has been observed that cancer cells can modify integrin expression after drug treatment, and this might lead to the development of resistance to a single antagonist and, paradoxically, to promotion of tumor growth. For instance, the FN-binding integrins αvβ3 and α5β1 are coexpressed on tumors and metastases, and each integrin regulates the functions of the other;[19,33,34] the inhibition of integrin αvβ3 can increase cancer invasiveness in the presence of high levels of FN, due to increased recycle of integrin α5β1, while inhibition of β1 integrins can promote tumor progression and metastasis by increasing the expression of β3.[35,36]

In any case, selective integrin ligands remain fundamental in order to explore on a rational basis the 3D disposition of the pharmacophoric groups (e.g. the guanidino and the carboxylate groups of the RGD sequence). This systematic approach was termed “spatial screening” by Kessler et al.[37] However, because of the close similarities between the structures of the different members of the integrin family, and between their respective ECM ligands, the design of selective peptide therapeutic agents represented a hard task.[38] Illustrative examples of receptor-specific ligands are shown in Figure 2. The cyclic hexapeptide **1** c[Arg-Gly-Asp-D-Phe-

Val-Gly], or c[RGDfVG], were the lower-case amino acid abbreviation encodes a D-configured residue, is an efficient inhibitor of FB binding to the integrin αIIbβ3, IC_{50} = 5.0×10^{-8} M, involved in platelet aggregation;[39] on the other hand, the cyclic pentapeptide **2** c[Arg-Gly-Asp-D-Phe-Val], or c[RGDfV], prevented binding of VN to the integrin αvβ3, IC_{50} = 4.9×10^{-8} M, playing a role in tumor cell adhesion, angiogenesis, and osteoporosis. The different receptor specificity of these antiadhesive compounds was correlated to the different 3D disposition of their pharmacophores. Conformational analyses showed that the RGD motif occupies the positions *i*+1 to *i*+3 of a β-turn in the αIIbβ3 selective hexapeptide **1** (Figure 2B), while it resides in the positions *i* to *i*+2 of a regular γ-turn in the αvβ3 selective pentapeptide **2** (Figure 2C).[37] However, although it is highly selective for αvβ3 vs αIIbβ3, **2** is not selective over other RGD-binding αv integrins.

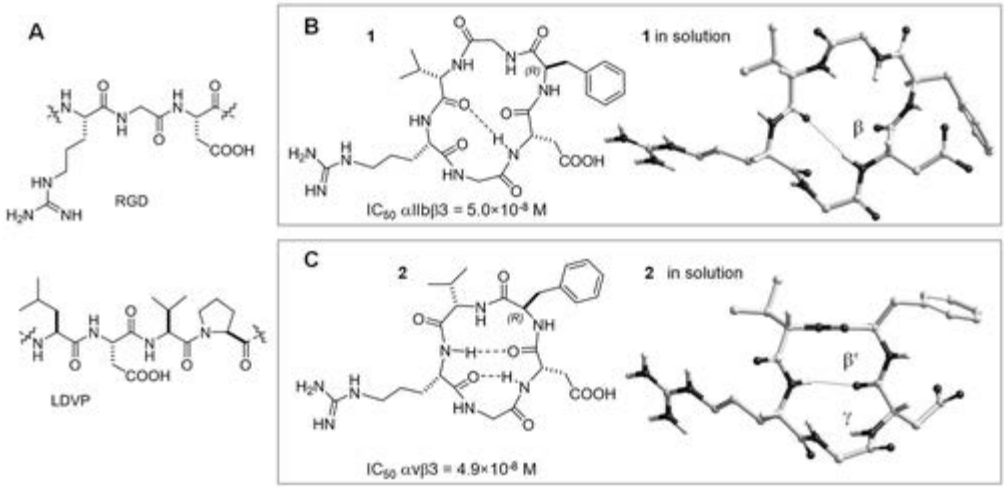

Figure 2 (**A**) The RGD and LDVP minimal binding motifs. (**B**) Structure and extended conformation in solution of **1**. (**C**) Structure and kinked conformation in solution of **2**. IC_{50} values refer to isolated integrins. The 3D structures were determined by two-dimensional NMR in combination with restrained and free molecular dynamics simulations.[37]

Kessler and coworkers also investigated the biological activity of retro (DGR), inverso (rGd), and retro-inverso (dGr) analogs (plus their stereoisomers) of the selective and superactive αvβ3 integrin inhibitor c[RGDfV] **2**.[40] Among the amino acid residues present in pentapeptide **2**, valine was found to be less important for binding αvβ3 and αvβ5 integrins.[37] For this reason, peptide c[RGDfK] become very popular since the lysine residue allowed to link the peptide over a length-optimized spacer and eventually to fluorescent tags, nanoparticles, or nanomaterials.[25,28,41]

Subsequently, each backbone amide segment in c[RGDfV] **2** was successively *N*-methylated to provide the monomethyl cyclopentapeptides. The effect of this derivatization on the activity was investigated, and revealed c[RGDf-*N*(Me)V] **3**, or cilengitide, as a highly active antagonist of the pro-angiogenic integrins αvβ3, αvβ5, and α5β1, with IC_{50} values of 0.65, 11.7, and 1.3×10^{-8} M, respectively (and a IC_{50} of 8.1×10^{-7} M for the integrin αIIbβ3), among the most potent ever developed,[42] subsequently investigated in clinical trials as an anticancer therapeutic.[43,44] In aqueous environment, **3** exists in a conformational equilibrium between two inverse γ-turns at Arg and Asp, and a γ-turn at Gly. The kinked backbone was identified as the most salient feature that differentiates αvβ3 and αIIbβ3 antagonists.

The structural basis for the binding of αvβ3 to c[RGDf-*N*(Me)V] (**3**) was disclosed by the analysis of the X-ray crystallographic structure of the extracellular portion of integrin αvβ3 in complex with **3**. The structure of the complex showed that the ligand is located at the interface between the αv and β3 subunits, resulting in extensive contact (Figure 3).[45] The αvβ3 integrin-c[RGDf-*N*(Me)V]-Mn^{+2} structure (PDB ID: 1L5G) revealed that the peptide is inserted into a crevice between the propeller and βA domains on the integrin head. The five Cα atoms of the cyclic peptide form a slightly distorted pentagon, and the side chains of Arg and Asp point to opposite directions. Strong ionic interactions bind the guanidinium group of Arg to Asp^{218} at the bottom of the groove, and to Asp^{150} at the backside. One of the Asp carboxylate oxygens is in close contact with the metal-ion-dependent adhesion site (MIDAS) in βA. The other carboxyl oxygen of Asp of the ligand is involved in hydrogen bonds with the amide protons of Tyr^{122} and Asn^{215}. Compared to the 3D model deduced by conformational analysis conducted in-solution for **2** and correlated cyclopeptides,[37,38,40] the solid model of **3** shows some differences, being characterized by two inverse γ-turns centered on Asp and Arg, and a less 'kinked' RGD arrangement.

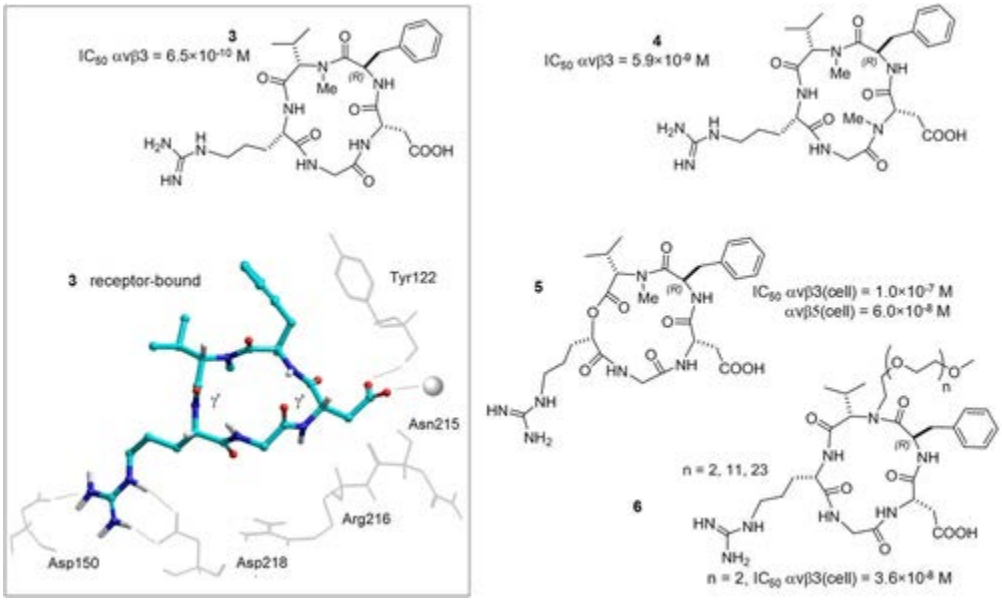

Figure 3 Structure c[RGDf-*N*(Me)V], cilengitide **3**; in the box: sketch of the main interactions of **3** with the *αvβ*3 binding site, as determined from the crystal structure of the complex (PDB ID: 1L5G); the ball represents a Mn2+ ion.45 Di-*N*-methylated **4**, depsi-analog of cilengitide **5**, and *N*-oligoethylene glycol substituted analogue **6**. IC50 values refer to isolated integrins or to integrin-expressing cells (cell).

The availability of the ligand-receptor X-ray crystallographic structure (see a sketch in Figure 3) gave the opportunity to analyze plausible candidate ligands by massive *in-silico* screenings, and to conduct highly detailed molecular docking analyses.[46] As for the other integrins, models of α5β1 integrin were initially developed by homology on the basis of the αvβ3 integrin-**3** complex structure,[47,48] or by binding pocket mapping,[49] and were subsequently utilized to perform molecular docking simulations to rationalize the structural requisites of ligand-receptor binding. In a similar way, homology models[50,51] or models derived from a combination of theoretical methods[52,53] were utilized to design potential ligands of integrin α4β1. Currently, high-resolution structural data are available also for the ectodomains of the integrin αIIbβ3[54,55] and of the integrin α5β1[56] in complexes with their respective RGD ligands. The "spatial screening" approach by Kessler and co-workers remains a fundamental step for the development of integrin ligand, but the conclusions derived from 3D conformational analysis not always agree with structural information provided by X-ray crystal structures of the integrins in complex with their ligands.

Since highly active and selective peptides are very useful tools to investigate the specific role of the integrin αvβ3 in angiogenesis and cancer, Kessler et al. proposed di-*N*-methylated analogues of **3**. The di-methylation of the backbone consented to fine-tune the biological activity of the cyclic RGD sequences by stabilizing

αvβ3-specific bioactive conformations. In particular, the cyclopeptide c[RG-*N*(Me)D-f-*N*(Me)V] **4** (Figure 3) retained a nanomolar αvβ3-integrin binding affinity, IC_{50} = 5.9×10^{-9} M, but highly reduced activity for integrins αvβ5 and α5β1, with IC_{50} values > 3×10^{-6} M, and 2.7×10^{-7} M, respectively, and a $IC_{50} > 1\times10^{-6}$ M for the integrin αIIbβ3.[57]

The structure of the prototypic ligand cilengitide **3** was the object of numerous modifications. For instance, Albericio et al. synthesized all five depsi-analogues of cilengitide by introduction of α-hydroxy acid residues in place of the normal amino acids. The analogue **5** (Figure 3) with ester link between *N*-Val and Arg showed increased potency with respect to the parent compound, being a potent small-molecule dual αvβ3 and αvβ5 antagonist in cell adhesion assays, IC_{50} αvβ3/FN = 1.0×10^{-7} M, IC_{50} αvβ5/VN 6.0×10^{-8} M, respectively, compared to IC_{50} = 3.2×10^{-7} M and 2.0×10^{-7} M for cilengitide under the same conditions.[58] As another example, the *N*-Me group was replaced by *N*-oligoethylene glycol (N-OEG) of increasing length to provide the more lipophilic bioactive analogues **6** (Figure 3).[59]

3. Integrin ligands with β-amino acid residues external to the recognition motifs

The rational design of integrin-selective peptidomimetic antagonists requires the precise prediction of the 3D structure. Herein we review the targeted incorporation of β-amino acids positioned externally to the recognition motif (e.g. RGD), and the consequent effects they exert on the geometry of peptide backbone. It has been shown that the β-amino acidic building blocks tend to adopt preferential conformations, and act as inducers of bioactive secondary structures. These findings can be utilized for designing peptidomimetic antagonists, since the specific 3D display of the pharmacophoric groups can be pre-defined by incorporation of tailor-made β-amino acids at a certain positions of the sequence.

3.1. Ligands with acyclic external β-amino acids or their mimetics

Sewald and coworkers have questioned whether cyclopeptides composed of both α- and β-amino acids may display distinct conformational preferences. In order to solve this question, the conformational impact of

the incorporation of a β-amino acid in model cyclopeptides was investigated by a systematic permutational replacement of one α-amino acid by the corresponding β^3-analogue.[60] The cyclic pentapeptide c[Arg-Gly-Asp-D-β-Phe-Val] **7** (following Seebach's nomenclature,[6] β-Phe in **7** corresponds to β^3-Phenylglycine, β^3-Phg) showed an high affinity for isolated αvβ3 integrins, $IC_{50} = 2.5\times10^{-9}$ M, but in addition inhibited αIIbβ3 integrin-mediated thrombocyte aggregation with an IC_{50} value of 7×10^{-6} M, comparable to that of the reference cyclohexapeptide **1**. It can be appreciated that the β-amino acid residue is located at the central position of a tight inverse turn closely related to a γ-turn (Figure 4), namely a geometry whose dihedral angles can be correlated to a γ-turn conformation, the only difference being the insertion of a CH_2 into the peptide backbone (*pseudo* γ-turn). The authors observed that the superposition of the in solution-conformations of **1** and **7** reveal a satisfactory overlay of the peptide backbones and of the Cα-Cβ vectors, accounting for the similar antagonist activities of the two peptides. On the other hand, pentapeptide c[Arg-Gly-Asp-D-Phe-β-Leu] **8** (β-Leu corresponds to β^3-Val using Seebach's nomenclature[6]) presents a βII'-turn centered on Gly-Asp, with β-leucine placed in the central position of a *pseudo* γ-turn, suggesting that a β-amino acid may impose a stronger conformational control respect to a D-amino acid. This peptide showed improved affinity for isolated αvβ3 integrins, $IC_{50} = 9.6\times10^{-10}$ M, and reduced efficacy against thrombocyte aggregation, $IC_{50} = 3.2\times10^{-5}$ M.

Subsequently, Sewald et al. extended their studies to cyclotetrapeptides (CTPs) containing a β-amino acid residue, by introducing in c[RGDfV] **2** the β-amino acid D-β-Phe in place of the dipeptide D-Phe-Val. The cyclotetrapeptide **9** so obtained showed nanomolar affinity for the isolated integrin αvβ3, $IC_{50} = 6.3\times10^{-8}$ M, and a remarkable selectivity over αIIbβ3, $IC_{50} > 3\times10^{-4}$ M. The β-amino acid residue is found in the central position of the pseudo γ-turn, thus inducing formation of the required γ-turn centered on Gly of the RGD motif (Figure 4). The conformation of ligands **2** and **9** seems indeed comparable and adequate for proper interaction with integrin αvβ3 within the pharmacophoric regions.

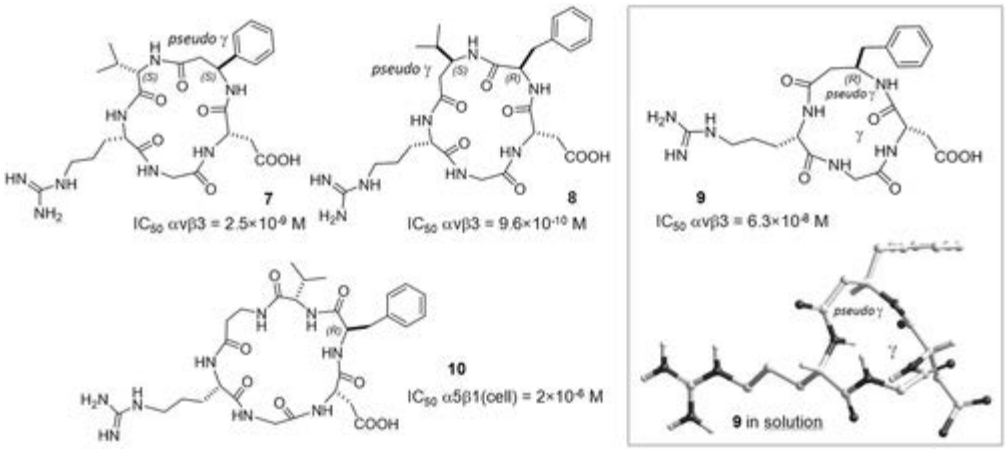

Figure 4 Cyclopentapeptides **7** and **8**. In the box: the cyclotetrapeptide *αvβ*3 antagonist **9**, rationally designed by incorporation of a *β*-amino acid as a pseudo *γ* -turn inducer; the RGD sequence forms a complementary *γ* -turn; 3D structure of **9** determined by 2D NMR, distance geometry, and restrained molecular dynamics simulations.60 Cyclohexapeptide *α*5*β*1 antagonist **10**. IC50 values refer to isolated integrins or to integrin-expressing cells (cell).

These preliminary results support the initial hypothesis that β-amino acids can act as inducers of *pseudo* γ-turns, allowing for the control of the peptide's backbone conformation, and consequently of the spatial orientations of the pharmacophoric groups of the RGD sequence.

The strategy was extended to the preparation of cyclic RGD peptides specifically designed for their affinity towards the integrin α5β1. In particular, Sewald and co. synthesized a library of peptide sequences containing β-amino acids as inducers of the desired conformations. This search led again to the cyclopentapeptide **8**, and to the new cyclohexapeptide c[Arg-Gly-Asp-D-Phe-Val-β-Ala] **10** (Figure 4), low-micromolar inhibitors of the attachment of the α5β1 integrin-expressing K562 cells to FN, with IC_{50} values of 3×10^{-6} M and 2×10^{-6} M, respectively, compared to $IC_{50} = 2.8\times10^{-4}$ M for the reference compound c-[Arg-Gly-Asp-D-Phe-Val] **2**.[61] From the conformational analysis of the structure in solution of the peptide, it was concluded that a short average distance between the Cβ of Arg and Asp is required for binding to α5β1.

Generally, cyclopenta- and cyclohexapeptides are easy to prepare, but their large rings imply high backbone flexibility. On the other hand, the smaller CTPs can be considered the minimal turn-mimics among the cyclopeptides. Unfortunately, CTPs composed of all α-amino acids are difficult to obtain, and frequently show mixtures of *cis*/*trans* isomers of the peptide bonds. Nevertheless, the incorporation of a distinct β^3- or β^2-amino acid residue in the sequence of the CTP can improve the yield of cyclization, and can stabilize the *all-trans* peptide bond conformation.[60,62,63]

In this context, partially retro cyclotetrapeptides (PR-CTPs) were proposed by Gentilucci et al.[64] as easily available CTP mimetics characterized by alternative secondary structures with respect to common CTPs (Figure 5). The cyclic structure and the presence of peptide bond surrogates was expected to improve enzymatic stability and molecular lipophilicity. The combination of *in vivo* stability and ability to cross biological compartments can strongly increase the bioavailability of drug leads based on these scaffolds. The stereoisomeric 13-membered PR-CTPs c[β-Xaa-*ψ*(NHCO)Ala-*ψ*(NHCO)Gly-Phe], containing a 1,2-diamine fragment as a β^2-homo amino acid equivalent, were analyzed as models (Figure 5). The notation *ψ*(NHCO) has been proposed to indicate the occurrence of a retro peptide bond between two consecutive amino acids, i.e. -NH-C(O)- instead of the normal -C(O)-NH-.[65,66] This implies that in cyclic partially retro peptide the first amino acid of the modified sequence is converted into a diamine and the last one is converted into a diacid (Figure 5).

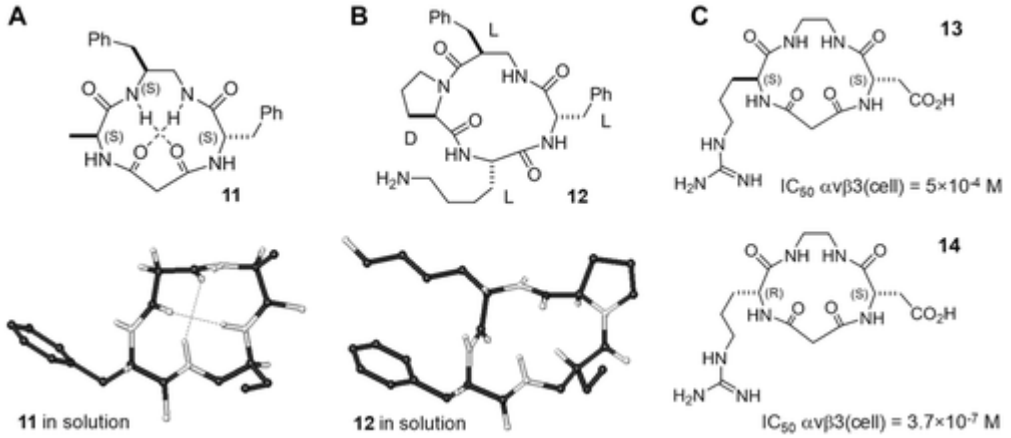

Figure 5 (**A**) Structure and backbone conformation of c[*β*-Phe-*ψ*(NHCO)Ala-*ψ*(NHCO)Gly-Phe] **11**.64 (**B**) Structure and conformation of c[(*S*)-*β*2-Phe-D-Pro-Lys-Phe] **12**.63 Conformations determined by 2D NMR and molecular dynamics; some side chains have been omitted for clarity. (**C**) Structures of PR-CTP RGD mimetics **13**, **14**. IC50 values refer to integrin-expressing cells (cell).

Conformational analysis of the PR-CTPs models containing an unsubstituted diamine revealed certain backbone flexibility, especially in the diamine region, whereas PR-CTPs that incorporated a substituted diamine segment (e.g. **8**, Figure 5A) were much more rigid. In order to check if the PR-CTPs might represent novel 3D scaffolds respect to the 13-membered CTPs already reported in the literature, the conformations of c[β-Phe-*ψ*(NHCO)Ala-*ψ*(NHCO)Gly-Phe] **11** (Figure 5A), and c[(*S*)-β^2-Phe-D-Pro-Lys-Phe] **12**, reported by Arvidsson et al.[63] (Figure 5B) were compared.[67] These peptides share the same stereochemistry pattern: the (*S*)-diamine portion of **11** replaces the (*S*)-β^2-Phe residue in **12**, L-configured Ala in the PR-CTP **11**

corresponds to the D-configured Pro in the normal peptide, and the malonyl moiety ψ(NHCO)Gly adopts a conformation which is consistent to a D-amino acid residue. Nevertheless, the comparison of the two structures confirms that the two scaffolds are topologically non-equivalent (Figure 5), owing to the different hydrogen bonds, the position of the β-Phe side chain, below the macrocycle plane in **12** and above the plane in **11**, and because of the *cis* β-Phe-D-Pro ω bond in **12**.

The PR-CTPs were utilized for preparing the cRGD analogues c[β-Ala-ψ(NHCO)Asp-ψ(NHCO)Gly-Arg] (**13**) and c[β-Ala-ψ(NHCO)Asp-ψ(NHCO)Gly-D-Arg] (**14**) (Figure 5C), which were assayed as inhibitors of the adhesion of the native ligand FN to SK-MEL-24 (human malignant melanoma) cells, expressing the integrin αvβ3. The IC_{50} values of **13** and **14** were 5×10^{-4} M and 3.7×10^{-7} M, respectively, clearly indicating that the different PR-CTP RGD possess distinct biological activities.[64]

Moving from these preliminary results, the stereoisomers of the PR-CTP sequence c[β-Phe-ψ(NHCO)Ala-ψ(NHCO)Gly-Phe] were analyzed as topology models having the three side chains directed towards precise directions. The topographic features of the eight PR-CTP models can be rendered using the Dunitz-Waser simplification concept (Figure 6).[68] The Dunitz-Waser concept was developed for cycloalkenes and has postulated that a *trans* double bond can be substitute by a long bond and a *cis* double bond by a phantom atom to understand the dynamics of cycloalkenes. This concept was translated into cyclic peptides by considering a peptide bond equivalent to a C=C double bond.[69]

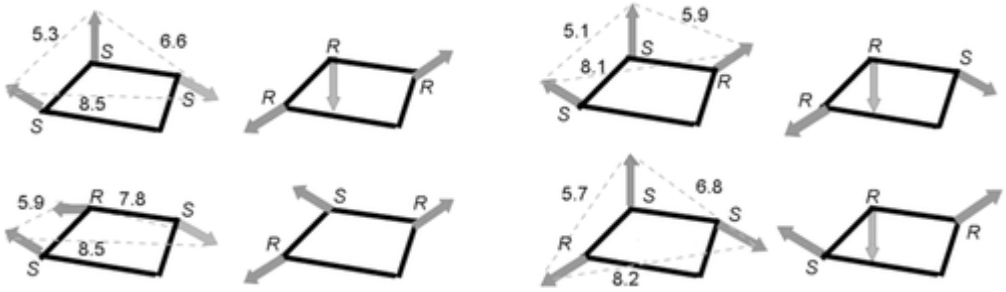

Figure 6 Schematic Dunitz–Waser topographic depiction of the eight PR-CTP models (enantiomeric pairs), showing the *S*/*R* stereochemistry of the C*α*, and the distances (° A) between the C*β* atoms. Gray arrows indicate the pseudo-axial or pseudo-equatorial disposition of the side chains (C*α*-C*β* vectors).

All stereoisomers show a strong preference for a secondary structure characterized by a β-turn centered on β-Phe-ψ(NHCO)Ala, and a second one on Phe-β-Phe-ψ(NHCO).[70] This feature correlates to the strong tendency of the diamine amide protons to participate to H-bonded structures. This observation is not obvious;

indeed, literature precedent suggested that configurational changes in a cyclopeptide can lead to alternative secondary structures.[37,40,60,62,63] Besides, it can be appreciated that the stereoisomeric scaffolds actually differ in the directions of the Cα-Cβ vectors of Ala, diamine, and L/D-Phe.

The eight stereoisomers of the PR-CTP sequence c[β-Phe-ψ(NHCO)Asp-ψ(NHCO)Gly-Arg] containing 3-phenylpropane-1,2-diamine (a β-Phe retro-mimic), and a malonate (a retro-Gly), were synthesized. The ability of the resulting compounds to inhibit the adhesion of the α5β1 integrin-expressing K562 cells (human erythroleukemic cells) or αvβ3 integrin-expressing SK-MEL-24 cells to immobilized FN, as well as the adhesion of αvβ3 integrin-expressing HUVEC cells (human umbilical vein endothelial cells) to immobilized VN, was evaluated. Compound **15**, c[(*R*)-β-Phe-ψ(NHCO)Asp-ψ(NHCO)Gly-Arg] (Figure 7), containing (*S*)-Arg and (*S*)-Asp, exhibited the highest potency as an inhibitor of cell adhesion mediated by αvβ3 and α5β1 integrins.[71] The observed IC_{50} value for α5β1 integrin/FN (K562 cells) was 2.4×10^{-8} M, that is about 10 times lower than that exhibited against αvβ3 integrin, IC_{50} αvβ3/FN (SK-MEL-24 cells) = 1.8×10^{-7} M, IC_{50} αvβ3/VN (HUVEC cells) = 2.4×10^{-7} M. The diastereoisomer **16**, c[(*S*)-β-Phe-ψ-(NHCO)Asp-ψ(NHCO)Gly-Arg] (Figure 7), differing from **15** exclusively by the configuration of the diamine moiety, maintained sufficient affinity for α5β1 integrin, but increased selectivity against αvβ3 integrin. Indeed, although **16** exhibited an IC_{50} α5β1/FN value of 5.2×10^{-7} M, its activity toward αvβ3 integrin dropped to IC_{50} αvβ3/FN = 1.1×10^{-5} M and IC_{50} αvβ3/VN = 2.5×10^{-5} M.

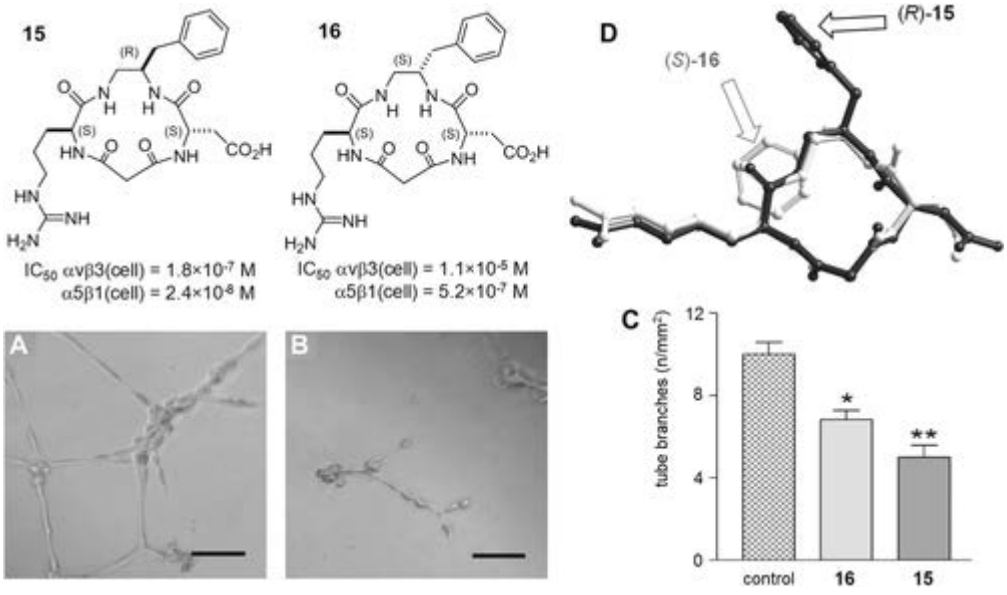

Figure 7 Structures of the PR-CTP RGD mimetics **15** and **16**; IC50 values refer to integrin-expressing cells (cell). (**A** and **B**) The $\alpha 5\beta 1/\alpha v\beta 3$ mixed integrin antagonist **15** inhibits bFGF-induced formation of capillary-like tubes of HUVEC on Matrigel; (**A**) HUVEC plated on Matrigel in the presence of bFGF; (**B**) HUVEC treated with compound **15** (1 μM), black bar = 100 μm. (**C**) Mean numbers of tubes per square millimeter ± SEM; $*P < 0.01$, $**P < 0.05$ vs. control (Newman–Keuls test after ANOVA). (**D**) Overlap of the backbone structures of **15** (black) and **16** (gray), determined by ROESY and molecular dynamics.[71]

The potential antiangiogenic activity of these novel antagonists of the integrins α5β1 and αvβ3, was estimated *in vitro* by analyzing the formation of capillary tubes composed of HUVEC cells cultured in Matrigel, when stimulated by basic Fibroblast Growth Factor (bFGF). HUVEC cells plated in the presence of bFGF alone gave rise to a nice capillary-like network (Figure 7A). The bFGF-stimulated formation of the capillaries was significantly inhibited by compounds **15** and **16** (for compound **15**, see Figure 7B). The number of tube branches per square millimeter was reduced from 10 ± 3 (bFGF-treated HUVEC) to 5.1 ± 0.7 by treatment with 1 μM **15** and 6.8 ± 0.9 with 1 μM **15** (Figure 7C).

The biological activities of **15** and **16** appear somewhat contrasting, despite the fact that the amino acid sequence of the peptides is identical. Conformational analysis was performed and confirmed the side chains 3D display as predicted from the corresponding 13-membered PR-CTPs models (Figure 6). The two stereoisomers share the same disposition of the RGD-mimetic region. The average distance between the β carbons of Asp and Arg, (~8.5 Å), and the distance between the carboxylate and guanidino groups (~13.5 Å), are very similar to that found in the α5β1 or αvβ3 selective RGD-cyclopeptides described in Section 2. The most relevant 3D difference can be noticed in the diamine region; apart from the different position of diamine amide protons, the benzyl side chain of the diamine is nearly equatorial in **15,** while it adopts an opposite axial position in **16** (Figure 7D).

The different αvβ3 receptor affinities were rationalized with the aid of docking studies performed on the model of binding site derived from the crystallographic structure of the extracellular segment of integrin αvβ3 in complex with cilengitide **3** (PDB ID: 1L5G).[45] The combination of conformational analyses and molecular docking support the fundamental role of the aromatic ring adjacent to Asp in determining the different pharmacological profile. Indeed, the pseudo-equatorial benzyl group in **15** points toward the outside of the αvβ3 integrin binding site, preventing any steric hindrance, and reproducing the orientation present in cilengitide. By contrast, in compound **16** the axial position of the aromatic side

chain is responsible for an unfavorable steric interaction that prevents the compound from entering into the receptor site (Figure 8).

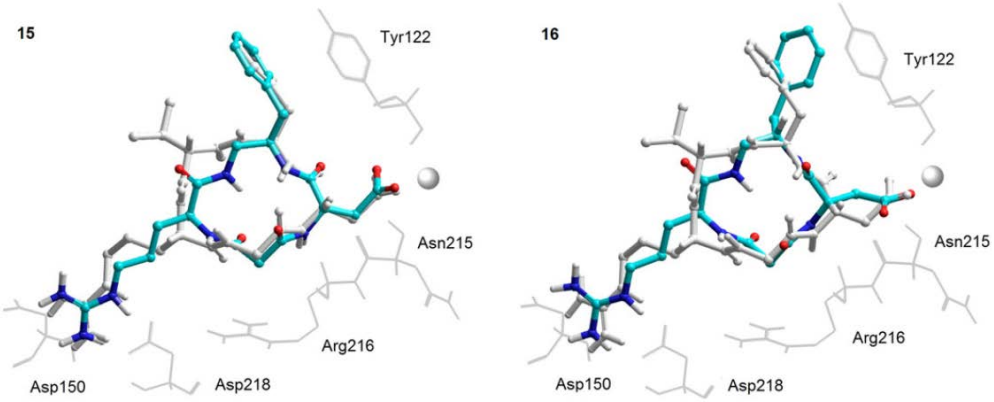

Figure 8 Sketches of the structures of **15** and **16**71 determined by molecular docking (Glyde version 4.5) of the ligands within the crystal structure of the integrin $\alpha v\beta 3$ (PDB ID: 1L5G).[45]

As for the integrin α5β1, at that time the 3D crystal structure was not available yet, and few details about ligand-receptor interactions were reported in the literature. However, a homology model of the receptor[47] was developed and utilized to design selective α5β1 integrin ligands.[48] On the basis of this model, it was postulated that the integrin α5β1 could host the benzyl side chain of both compounds. Indeed, the comparatively larger binding site of α5β1 integrin compared to that of integrin αvβ3 can easily accommodate the axial phenyl ring of **16**, leading to a pronounced selectivity for α5β1 over αvβ3 integrin, while the equatorial disposition of **15** can fit both integrins.

The better αvβ3 integrin receptor affinity of (*S*,*R*,*S*)-PR-CTP **15** respect to the (*S*,*S*,*S*)-configured **16** nicely confirms the predictive efficacy of the PR-CTP topographic models discussed above. The positioning and the distances between Cβ were correlated to the distances found in the bioactive conformation of the prototypic αvβ3-selective cilengitide **3**, discussed in the previous sections (Figure 9A). The comparison highlighted the good match between the topographic Dunitz-Waser depictions of **3** (Figure 9B) and of the (*S*,*R*,*S*)-CTP model (Figure 9C), and the poor overlap with the sketch of (*S*,*S*,*S*)-CTP concerning the benzyl side chain (Figure 9C).

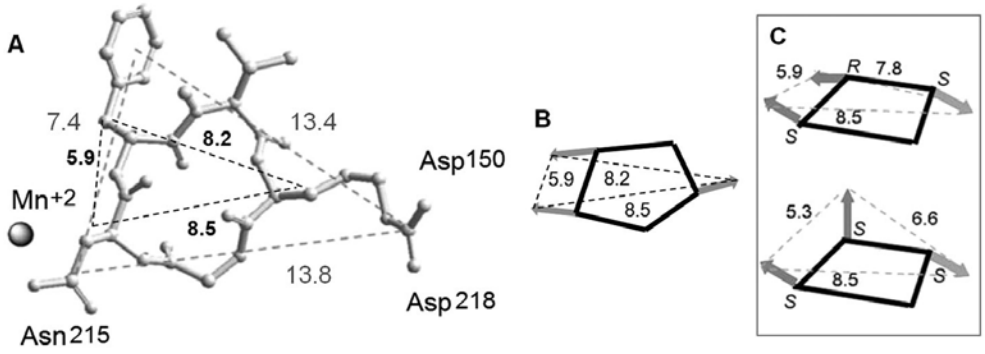

Figure 9 (**A**) Bioactive conformation of the *αvβ*3-selective c[RGDf(*N*-Me)V], cilengitide **3**, showing the distances (A°) between the pharmacophores (gray digits and gray dashed lines) and between C*β* atoms of Asp, D-Phe, and Arg (black digits and black dashed lines). (**B**) Dunitz–Waser sketch of **3**. (**C**) Dunitz–Waser sketches of (*S*,*R*,*S*)-CTP (top), and (*S*,*S*,*S*)-CTP (bottom), models of **15** and **16**, respectively.

3.2. Ligands with external cyclic scaffolds of β-amino acid structure/span

A few years ago, Sewald and coworkers reported the synthesis, the pharmacological evaluation, and structural determination, of several novel ligands for integrin αvβ3, including the pentapeptides c[Arg-Gly-Asp-(+)-β-Acc-Val] (**17**) and c[Arg-Gly-Asp-(−)-β-Acc-Val] (**18**) containing enantiomeric (+)- or (-)-*cis*-β-amino cyclopropanecarboxylic acid (β-Acc) adjacent to the RGD motif.[72] The biological activity of peptides **17** and **18** was determined in adhesion experiments with cancer cell lines. Peptide **17**, containing (+)-β-Acc, displayed a ten-fold higher affinity (IC_{50} = 2.0×10^{-8} M) than the reference peptide c[RGDfV] **2**, as determined by adhesion experiments of WM115 cells to VN. By contrast, the inhibitory effect of the diastereomeric **18** was comparable to that of **2**. The adhesion of K562 cells mediated by α5β1 integrin to FN was inhibited to nearly the same extent by peptides **17** and **18**, with IC_{50} values of 1.5×10^{-6} M and 1.8×10^{-6} M, respectively; that is, more active than reference peptide **2**.

The significantly different affinity of the β-Acc-RGD peptides to αvβ3 integrin can be interpreted as a consequence of the stereochemistry of the β-Acc residue. Conformational analysis revealed that in **17** glycine is located in the central position of a γ-turn, while the (+)-β-Acc residue occupies the *i+1* position of a *pseudo* β-turn (Figure 10). In peptide **18**, Asp is in the central position of an inverse γ-turn. Between the amino acids (-)-β-Acc and Gly, the structure adopts the torsional angles characteristic of a 3^{10} helix, thus corresponding to a conformation formerly known as the βIII turn with valine in the *i+1* position and arginine in the *i+2* position

(Figure 10). All this accounted for a more extended geometry of the RGD sequence for **18** relative to **17**, so the latter is more compatible with the structural requirements for optimal binding to integrin αvβ3 (Section 2), namely a short distance between the Cβ atoms of Arg and Asp of about 6.5-8.5 Å.

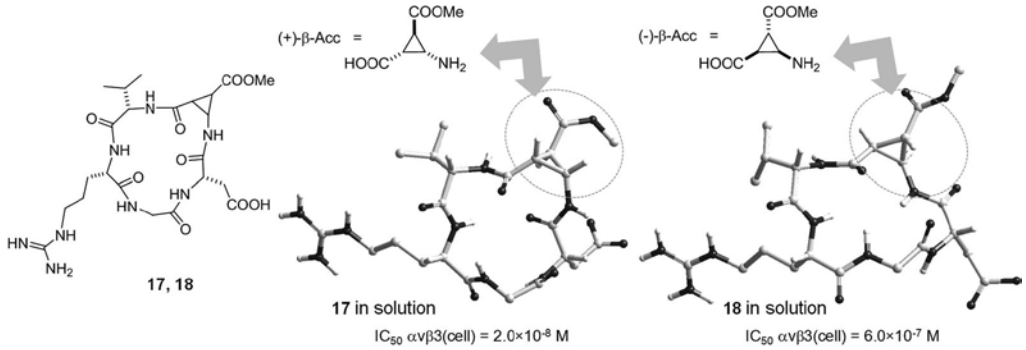

Figure 10 Structures of the (+)- and (-)-*β*-Acc, and *β*-Acc-containing peptides **17** and **18.** Lowest-energy conformations obtained by restrained MD calculations based on experimental C-C bond distance information. IC50 values refer to integrin-expressing cells (cell).

Albericio, et al. reported the efficient solid phase preparation of cyclic RGD peptides, connected 'head-to-tail' by the side chains of a diketopiperazine (DKP) rigid scaffold, giving rise to a new class of bicyclic RGD peptides. The DKP scaffold was obtained in solid phase by cyclization of a dipeptide orthogonally protected at the side chains, H-Lys(N^{ε}-Mtt)-Asp(βAllyl)-OMe, attached to a Backbone Amide Linker (BAL) resin by the peptide bond nitrogen. The affinity of the RGD-containing ligands comprising five to seven residues towards the αvβ3 integrin was determined in binding assays using the radioligand [^{125}I]echistatin. Results indicated that the compound which contained just the sequence RGD and the scaffold showed the highest binding affinity.[73]

In this context, some years later Piarulli, et al. developed a similar bifunctional DKP scaffold. The six-membered heterocyclic ring was prepared from (*S*)-2,3-diaminopropionic acid and L-aspartic acid (Figure 11); therefore, this scaffold includes two vicinal β-amino acids, namely a α,β^2-diaminoacid and a β-carboxy-β^3-amino acid.

The RGD sequence was coupled to either *cis*-DKP or *trans*-DKP (Figure 11). Following macrolactamization, the resulting cyclic RGD peptidomimetics **19** (*cis*-DKP) and **20** (*trans*-DKP) were examined *in vitro* as inhibitors of biotinylated VN binding to αvβ3 and αvβ5 receptors.[74] Interestingly, **20** exhibited a nanomolar affinity for the αvβ3 integrin, IC_{50} = 3.2×10^{-9} M, and 40-fold selectivity over αvβ5,

while **19** showed only a modest micromolar affinity for the αvβ3 integrin and no activity towards αvβ5 integrins, IC_{50} = 3.9×10^{-6} M.

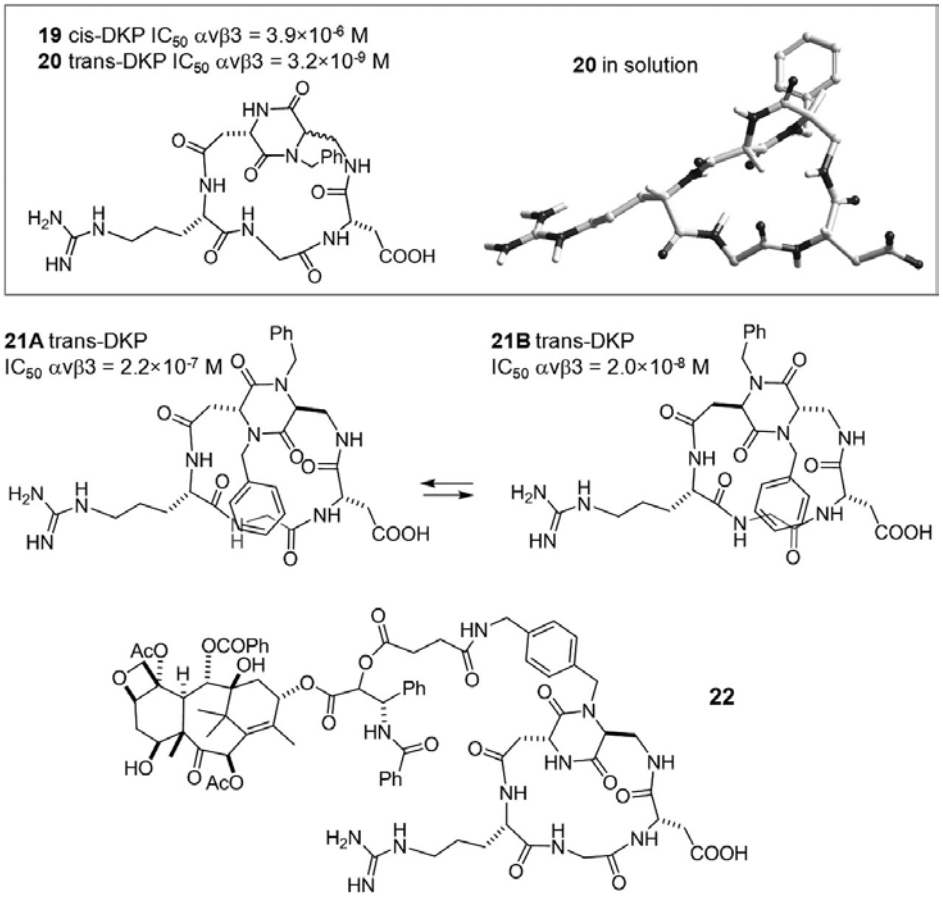

Figure 11 In the box: structures of cyclic RGD-peptidomimetics **19** and **20** containing diketopiperazine scaffolds, and 3D structure of **20** as obtained by restrained Monte Carlo/Stochastic Dynamics (MC/SD) simulations based on experimental bond distance information, showing a pseudo *β*-turn at DKP-Arg. Diastereomers **21A** and **21B**, resulting from hindered rotation. Structure of the c[DKP-RGD]-paclitaxel conjugate **22**. IC50 values refer to isolated integrins.

The different performance of the DKP-RGD-mimetics **19** and **20** was investigated by NMR spectroscopy and computational methods. Conformational analysis revealed that **19** exists as two interconverting conformers; NOESY spectrum showed two mutually exclusive long-range NOE contacts, one indicative of a conformer characterized by a β-turn centered on Gly-Asp, and a second one showing a β-turn centered on Arg-Gly. Conversely, the conformation of the RGD-mimetic **20** containing the *trans*-DKP is rather rigid, with a clear β-turn on DKP-Arg stabilized by a H-bond between Gly-NH and C5=O (Figure 11), and a distance between the Cβ of Arg and Asp of 9.4 Å. Docking computations of this extended conformation of **20** afforded a lowest-energy conformer that preserves the ionic interactions of cilengitide **3** in complex with integrin

αvβ3.[45] By contrast, the docked geometries of **19** produced top-ranked poses conserving optimal interactions only with the α subunit.

Subsequently, the Gennari group expanded the library of RGD mimetics by introducing the DKP scaffolds of differing configuration at the two stereocenters, as well as different *N*-substitution patterns. Eight resulting cyclopeptides were analyzed as inhibitors of the binding of biotinylated VN to integrins αvβ3 and αvβ5. The peptidomimetics derived from *trans*-DKPs gave nanomolar IC_{50} values.[75] Interestingly, the 2:1 **21A**:**21B** diastereomeric/rotamer pair was separated owing to hindered rotation of the dibenzyl-DKP scaffold (Figure 11). Poor receptor affinity was obtained for ligand **21A**, IC_{50} αvβ3 = 2.2×10^{-7} M, while rotamer **21B** was the most potent ligand of the series, IC_{50} αvβ3 = 2.0×10^{-8} M).

It was established that rotamer **21B** adopts a variety of conformations in solution, including an H-bonded type I β-turn having Gly-Asp at the positions *i+1*, *i+2*, characterized by an extended RGD sequence. Docking calculations starting from this conformation gave top-ranked binding modes consistent to the bioactive conformation of cilengitide **3** within the integrin (see above).[45]

In order to investigate the binding epitope of the c[DKP-RGD] peptidomimetics to the integrins, NMR studies based on saturation transfer and detection of transferred NOEs were used for analyzing the ligands during their interaction with living cells known to express on their membrane the integrins αvβ3 (ECV304 bladder cancer cells) and αIIbβ3 (human platelets).[76] This technique was originally introduced by Meyer for applications in the integrin field.[77] Transferred NOEs can be recorded only when there is rapid exchange, this meaning that the binding should not be too high and only ligands with relative low binding affinities can be investigated. The Meyer group therefore used the integrin αIIbβ3 and a αvβ3 selective ligand with much lower affinity to the investigated integrin. The NMR results were supported by docking studies and were compared to the results of competitive αvβ3 receptor binding assays and competitive ECV304 cell adhesion experiments, and clearly confirmed that only those ligands with *trans*-RGD fragments are able to interact with both the α and β integrin subunits via an electrostatic clamp.

The c[DKP-RGD] ligands were exploited for integrin-mediated delivery of the cytotoxic drug paclitaxel (PTX).[78] The c[DKP-RGD]-PTX constructs were good integrin ligands *in vitro*, since they inhibited

biotinylated VN binding to the purified αvβ3 integrin receptor at low nanomolar concentration. Furthermore, when tested against a panel of human tumor cell lines (including the cisplatin-resistant IGROV-1/Pt1), they showed cytotoxic activity with efficiency similar to that of paclitaxel. In particular, the c[DKP-RGD]-PTX **22** (Figure 11) emerged as a candidate for *in vivo* testing, due to its good activity and stability under physiological conditions and in plasma. Compound **22** exhibited higher tumor-targeting activity compared to PTX alone against an IGROV-1/Pt1 human ovarian carcinoma xenotransplanted in nude mice.

4. Integrin ligands with β-amino acid residues in place of Asp

One of the larger β3 integrin antagonist classes employs β-amino acids to mimic the aspartate residue of the RGD mimetic. Structure-activity relationship (SAR) investigations have revealed the potent activity of agents which have substituents appended to both the α and β position of the β-amino acid units of these antagonists. Several clinical candidates targeting platelet αIIbβ3 and containing these β-amino acid units were evaluated clinically. Since the many integrin peptidomimetic ligands of this kind have been previously reviewed exhaustively,[23,38,79] the following sections report selected representative examples from the recent literature.

4.1. Recent examples of β-amino acid analogues of Asp, and their uses in medicinal chemistry

Simple β-alanines[80] or β-alanine derivatives carrying different substituents at the β position have been successfully applied in the synthesis of RGD mimetics.[79,81,82] Most ligands include aromatic substituents to mimic an Asp-Phe dipeptide,[83,84] but also other groups have been utilized (e.g. an alkyne[85]).

By far, the most widely used β-amino acid equivalent is diaminopropionate.[23,38,79] Very often, the α-amino group is utilized to introduce diverse types of substituents, e.g. aryl, sulfonyl,[86] arylsulfonyl[87] groups etc., in close proximity to the carboxylic acid pharmacophore. These aromatic groups were shown to contribute to receptor affinity thanks to an additional, energetically favorable "exosite" π-π interaction with Tyr178 of αv.[88]

One extraordinary advantage of diaminopropionate is the opportunity that it provides to conjugate the integrin ligand to nanoparticles, antibodies, lipids, fluorescent tags, among others,[27,28] or for oligomerization

of the ligand.[89] For instance, the diaminopropionate segment allowed conjugating an oligomeric peptidomimetic integrin αvβ3 antagonist to a monoclonal antibody (MoAb), in order to increase integrin αvβ3 receptor-binding avidity (Figure 12). The antibody moiety served as carrier of the antagonist **23** to target tumor-induced neovasculature.[90]

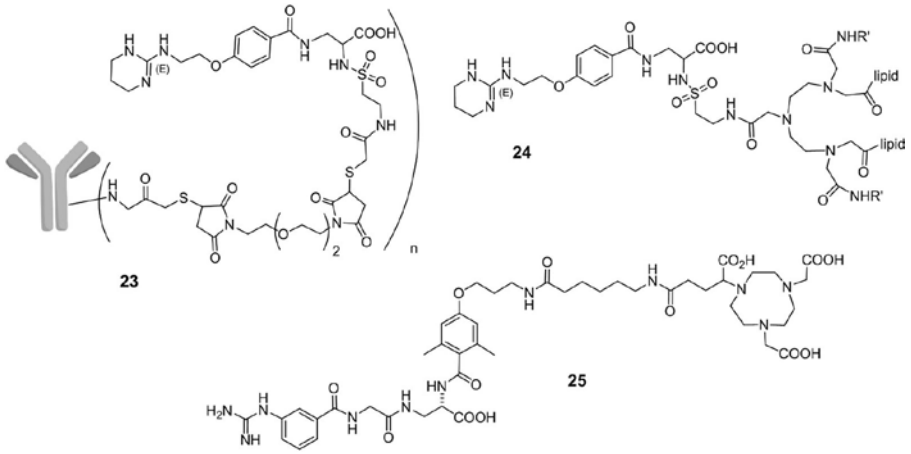

Figure 12 Structures of an integrin antagonist-conjugated MoAb **23**, a lipid-conjugated integrin antagonist **24**, and a NODAGA-conjugated integrin antagonist **25**.

The same αvβ3-targeting integrin ligand was coupled through the diaminopropionate unit to branched lipids **24** capable to form a cationic nanoparticle (Figure 12), in order to selectively deliver genes to angiogenic blood vessels in tumor-bearing mice.[91]

Kessler et al. functionalized a α5β1-selective antagonist (Figure 12) with 1-((1,3-dicarboxy)propyl)-4,7-(carboxymethyl)-1,4,7-triazacyclononane (NODAGA).[92] This strategy provided the compound **25**, an effective and selective α5β1-integrin antagonist that enabled specific molecular imaging *in vivo* by PET, based on the different integrin pattern of tumor cells.

The side-chain amino group of diaminopropionate was also functionalized to append biotin or a biotin derivative containing an oligo(ethylene glycol) ((EG)4) linker, to give a bifunctional RGD-based peptidomimetic particularly effective for surface presentation; the surfaces decorated with this ligand promoted both cellular adhesion and integrin activation.[93]

4.2. Retro-sequences containing *iso*Asp residues

Some researchers proposed that the spontaneous modification of the Asn-Gly-Arg (NGR) motif in FN ligands into *iso*DGR might result in a gain of integrins adhesion by creating a new binding site.[94,95] This hypothesis was critically examined using recombinant FN with mutations in the NGR motif.[96] Subsequent studies confirmed that the *iso*DGR sequence maintains the same binding mode of RGD, affording the classic electrostatic clamp, as well as the normal additional polar interactions.[97,98]

In this field, Kessler, et al. grafted the *iso*DGR motif onto the structures of retro-RGD cyclopentapeptides. The use of an *iso*Asp residue does not modify the span between the guanidinic and carboxylate pharmacophores; however, it provokes an enlargement of the macrocyclic peptide similar to that caused by the introduction of one β-amino acid (see Section 3.1). Specifically, from 15 bonds present in the normal cyclopentapeptides, the substitution leads to 16 bonds present in the *iso*DGR analogues. Therefore, this structural modification is expected to result in considerable conformational bias of cyclopentapeptide backbones.

On the other hand, binding experiments showed that the sequential position of the aromatic amino acid and glycine flanking *iso*DGR, determines the affinities of the pentapeptides to either integrin αvβ3 or α5β1. Indeed, c[phg*iso*DGRG] **26** (phg = D-phenylglycine) showed enhancement of pharmacological activity towards α5β1 integrin, IC_{50} α5β1 = 1.9×10^{-8} M as determined by competitive ELISA using immobilized ECM protein and soluble integrin, relative to integrin αvβ3 ($IC_{50} > 10^{-6}$ M).[99] By contrast, c[G*iso*DGRphg] **27** was more active towards integrins αvβ3 ($IC_{50} = 8.9\times10^{-8}$ M) (Figure 13). Molecular docking were performed for the αvβ3 receptor, using the crystal structure of the cilengitide-αvβ3 integrin complex, and the α5β1 receptor, starting from the homology model seen in Section 2.[45] The simulations confirmed the usual interaction patterns. Furthermore, selectivity toward FN-binding integrins α5β1 and αvβ6 relative to VN-binding integrins αvβ3 and αvβ5 was improved by appropriate substitution of the flanking amino acids in the peptide.[100]

Very recently, Gennari, et al. synthesized the cyclopeptides **28** and **29**, comprising *iso*DGR (Figure 13) and the bifunctional DKP scaffolds,[74,75] and determined their ability to compete with biotinylated VN for binding to the purified αvβ3 and αvβ5 receptors. In particular, compound **29** showed the lowest IC_{50} recorded value for integrins αvβ3 ($IC_{50} = 9.2\times10^{-9}$ M), and good selectivity over integrin α5β1.[101]

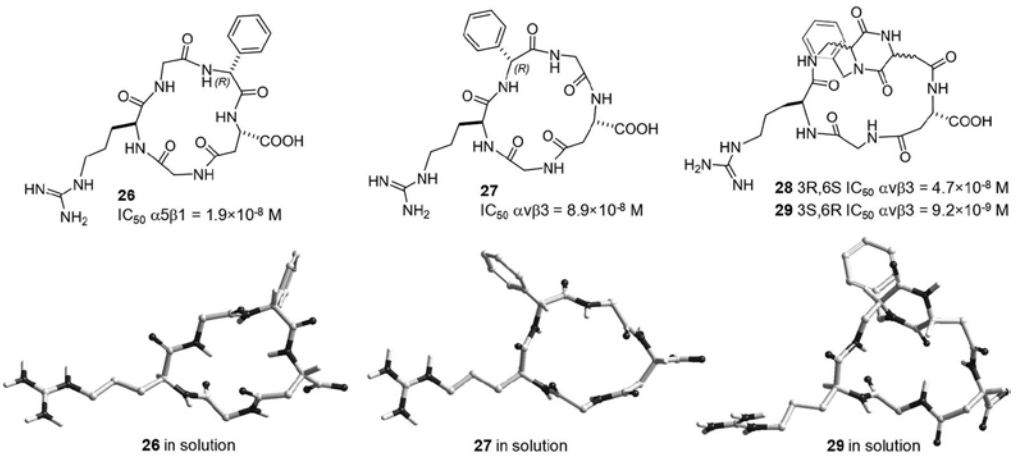

Figure 13 Structures of cyclic pentapeptides **26**, **27** containing the *iso*DGR motif, and of the cyclic *iso*DGR peptidomimetics **28** and **29** containing the bifunctional DKP scaffolds; 3D molecular structure of **26**, **27**,99,100 and *trans*-(3*S*,6*R*)-DKP-*iso*DGR **29**101 obtained by restrained MC/SD simulations based on experimental bond distance information, followed by energy minimization. IC50 values refer to isolated integrins

Data obtained from NMR experiments demonstrated the high conformational flexibility of compound **28**, while in the case of peptide **29**, experiments suggested the existence of two preferred conformations, a β-turn with a H-bond between DKP-NH10 and *iso*AspC=O, and a *pseudo* β-turn conformer stabilized by an H-bond involving Gly-NH and DKP-C5=O (Figure 13). Docking calculations confirmed that the latter structure corresponds to the bioactive conformation.

Finally, the *iso*Asp residue was also utilized both in straight or retro sequences by Gentilucci et al. in the preparation of conformationally constrained mimetics of the α4β1 integrin antagonist BIO1211 (see Section 5.2.2).[102]

5. Integrin ligands containing β-amino acid cores

A variety of cyclic (aromatic and non-aromatic) or acyclic scaffolds, with chiral and achiral structures, was examined to furnish Gly surrogates in RGD peptides.[22,23,38] Generally, only flat structures within the RGD mimetic permit to maintain the effective interactions with integrin receptors. Sugar and piperazine scaffolds which have shown poor or modest anti-αvβ3 activity, usually present almost flat structures, due to the all-equatorial conformations.[103,104,105,106] By contrast, replacement of the Gly residue by Ala, bulky, longer, or branched core residues, resulted in a dramatic loss in potency.[38,107] The introduction of β-amino acids or other β-amino acid derived moieties is expected to provide hybrid molecules with increased stability against

enzymatic hydrolysis. Clearly, the increased length of the β-amino acid relative to Gly impacts not only the distance between the pharmacophore-containing moieties, but also the conformations of the RGD tripeptide motif. For this reason, only peptidomimetic compounds specifically designed to maintain the correct shape and distances can successfully include a β-amino acid within the RGD sequence.

5.1. Integrin ligands containing acyclic β-amino acid cores

Some years ago, Hayashi et al. reported the potent non-peptidic αIIbβ3 integrin antagonist **30** (NSL-95301), with a unique trisubstituted β-amino acid unit utilized as central core. The β-amino acids were prepared from the corresponding β-lactams (Figure 14), prepared in turn by a convenient ester-imine condensation. Following conformational analyses and SAR studies, the optimization of the amidine group led to the potent and orally active antagonist of the platelet FB receptor **31** (Figure 14), containing 3-ethyl-2,2-dimethyl-β-alanine. The active (*R*)-enantiomer of **31** effectively inhibits platelet aggregation *in vitro*.[108] Tested *in vivo* in guinea pigs, **31** was orally active; the onset of antiplatelet action was rapid, albeit the duration was relatively brief.

The trisubstituted β-residue controls the active conformation of the molecule. Molecular modeling of **30** and related compounds revealed a quite rigid albeit linear structure, which effectively fixes the distance between the pharmacophoric ends. The amidino and the carboxyl groups project at opposite sides of a cup-shaped structure, the phenyl group at the β-position being perpendicular to the piperidine ring and amidinophenyl group. This cup-shaped rigid conformation originates from the correlated and restricted motions of the piperidine ring, the *geminal* groups at the α-position, and the β-substituent; the latter appeared to be very important to restrict the overall flexibility.

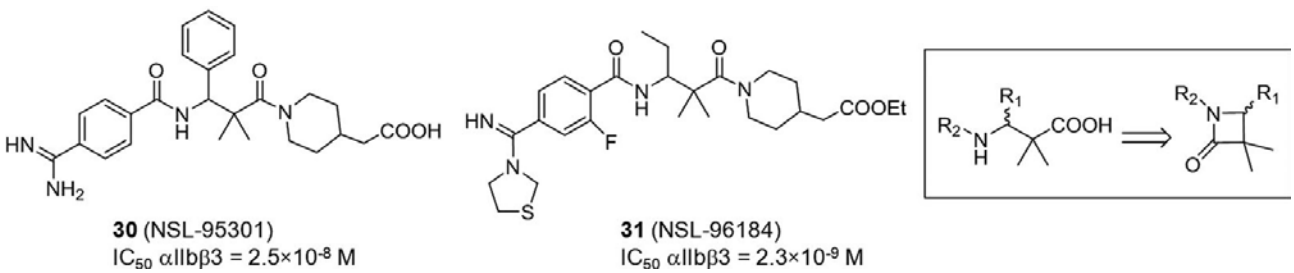

Figure 14 Structures of the αIIbβ3 integrin antagonists **30** and **31** containing the trisubstituted β-residues; in the box: retrosynthesis of the β-residues.

More recently, Cardillo, et al. reported the enantioselective transesterification or acylation of racemic β-amino esters by treatment with *Candida antarctica Lipase B* (CaLB)-catalyzed, for the isolation of enantiopure intermediates of pharmacological interest **32** and **33** (Figure 15). Both the malonyl and the β-amino esters proved to be suitable substrates for CaLB. The enzyme recognized under kinetic resolution conditions the less hindered position, and the transesterification reaction proceeded with good yields and high enantioselectivity. This strategy was applied to the two-step synthesis of the RGD mimetic compound **34**,[109] which showed moderate ability as inhibitor of cell adhesion mediated by integrins αvβ3 and α5β1, with IC_{50} values of 1.7×10^{-7} M and 9.7×10^{-7} M, respectively.[110]

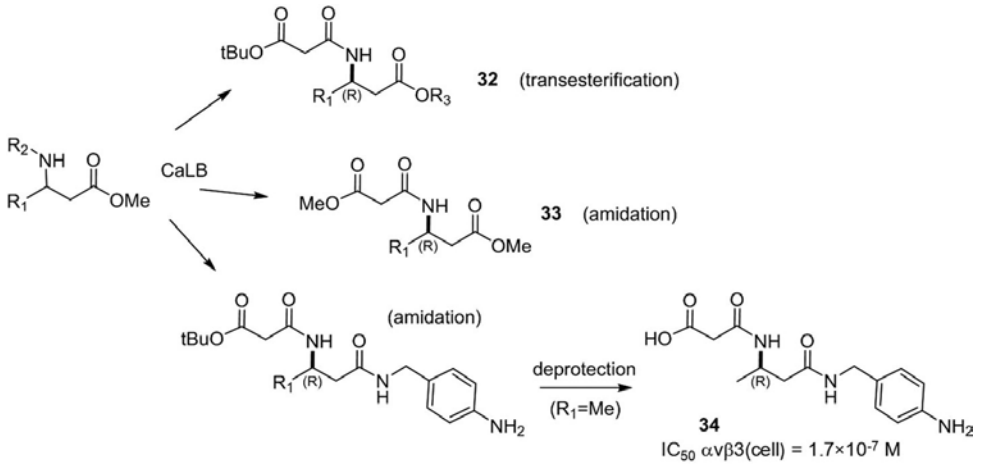

Figure 15 General strategies for obtaining sequences **32**, **33** containing enantiopure *β*-amino acids, including the RGD mimetic **34**, by CaLB-catalyzed resolution of racemic *β*-amino acid derivatives. IC50 value refers to integrin-expressing cells (cell).

Aiming at obtaining small mimetics of the RGD motif, Cardillo et al. introduced dehydro-β-amino acid as central scaffolds instead of Gly. Enantiopure allylic alcohols were prepared by an enzymatic approach, and the allylic amination of the deriving carbonates[111] with 4-substituted benzylamines proceeded through an SN2' mechanism (Figure 16A), giving access to a novel type of RGD mimetic requiring few protection-deprotection extra steps.[112]

Starting from racemic carbonates, Tolomelli, et al. prepared various RGD mimetic candidates and tested them in the inhibition of αvβ3 and α5β1 integrin-mediated cell adhesion.[113] The short molecules **35a-d** (Figure 16B) showed unexpected activity, and selectivity correlated to the substituent at position 3. Derivative **35a** (R

= Me) did not affect αvβ3 integrin-mediated cell adhesion, while it showed excellent inhibition of the α5β1 integrin (IC_{50} = 1.9×10^{-8} M). On the other hand, the compounds **35b** (R = *i*Pr) and **35c** (R = thiophenyl) had micromolar affinity toward both integrins, while **35d** (R = cyclohexyl) showed preferential affinity towards αvβ3 receptor. Nevertheless, the study of additional peptidomimetics is required before a clear understanding of SAR is reached. Moreover, these molecules are quite small relative to the usual RGD sequences, therefore the different side chains may be less determinant for integrin affinity. Few antagonists of similar length have been reported in the literature; for instance, the heterocyclic αIIbβ3 antagonist RUC-1 was shown crystallographically to bind only to the αIIb subunit, in contrast to classic RGD antagonists.[114] Docking analysis aimed at determining the binding mode of the short compound **35b** with the integrin αvβ3 were inconclusive. Indeed, the computations gave alternative plausible poses characterized by very similar docking scores, one showing ionic interactions with both the α (MIDAS) and β (Asp^{218}) subunits, plus a stacking interaction between the phenyl group of the ligand and Tyr^{178}, and a second pose in which the ligands maintain only the electrostatic interaction with MIDAS in the αv subunit.[115]

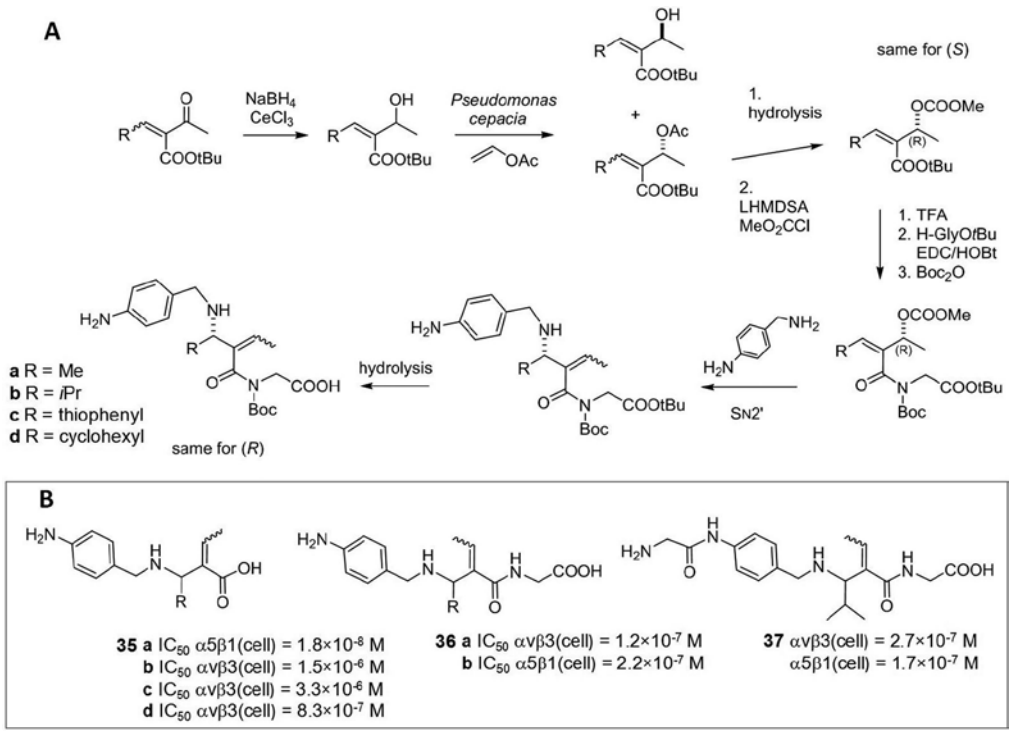

Figure 16 (**A**) Synthesis of enantiomerically pure allylic carbonates and synthesis of dehydro-*β*-amino esters through amination of allylic carbonates. (**B**) In the box: ligands **35**–**37** containing dehydro-*β*-amino acid scaffolds, examined for integrins *αvβ*3 and/or *α*5*β*1. IC50 values refer to integrin-expressing cells (cell).

The larger ligand **36b** with R = *i*Pr (Figure 16) exhibited an increased α5β1 integrin-mediated inhibitory activity (IC_{50} α5β1 = 2.2×10^{-7} M; IC_{50} αvβ3 = 2.0×10^{-6} M) in comparison to the shorter analog **35b**. By contrast, compound **36a** with R = Me displayed good activity and a strong preference toward αvβ3 integrin (IC_{50} = 1.2×10^{-7} M). The molecule was further elongated by introduction of a second glycine unit (Figure 16); this modification afforded the most potent dual antagonist **37** (IC_{50} αvβ3 = 2.7×10^{-7} M; IC_{50} α5β1 = 1.7×10^{-7} M).

The effect of the most effective compounds **36a** and **37** on intracellular αvβ3 integrin-mediated signaling activation was assessed using DAOY medulloblastoma cells. Pre-incubation with both compounds produced a measurable decrease of the phosphorylation of extracellular-signal-regulated kinases (ERK) induced by FN. In addition, the effect of both compounds on intracellular α5β1 integrin-mediated signaling activation was analyzed using K562 cells. Compound **37** reverted FN-induced phosphorylation of ERK1/2. By contrast, compound **36a** was not able to reduce ERK pathway activation, which is suggestive of a different mechanism of action.

The different performances of **36b** and **37** in αvβ3-mediated cell adhesion inhibition were analyzed by docking computations, using the X-ray crystal structure of the ectodomain of integrin αvβ3 complexed with the cyclic pentapeptide ligand cilengitide **3** (Section 2).[45] The pose of compound (3*R*,Z)-**36b** with the best docking score shows the carboxylate group coordinated to the divalent cation in the MIDAS region of the β3 subunit, while the ligand's aromatic amine interacts with the negatively charged side chain of Asp^{218} in the αv subunit. Nevertheless, for the latter moiety the fit with the cilengitide Arg guanidinium group is not precise. As for compound (3*R*,Z)-**37**, the introduction of an additional glycine gave the correct distance required for a good fit with the receptor. The best calculated pose of (3*R*,Z)-**37** showed the acid and basic pharmacophoric groups involved in strong ionic bonds with charged regions of the receptor binding site, nicely reproducing the electrostatic clamp of the RGD sequence of integrin-bound **3**.

5.2. Integrin ligands containing heterocyclic β-amino acid cores

One approach to obtain highly stable and structurally defined peptidomimetics is to incorporate a conformationally restricted residue, introducing a local constraint which may result in a significant reduction of the accessible conformational space.[116] In this context, a small-to-medium sized heterocycle can be incorporated as central core of a peptide, to orient the pharmacophoric side chains and to fix the adequate distanced for binding. Generally, heterocyclic scaffolds of minimal structural complexity and steric requirements have been designed to prevent undesired interactions. The following sections are dedicated to illustrative examples of integrin ligands containing a heterocyclic core having a β-amino acid structure. Representative experimental protocols are included to highlight salient synthetic procedures for the preparation of non-racemic scaffolds.

5.2.1. Integrin ligands containing β-lactam scaffolds

Claudio Palomo et al. proposed the use of peptides containing β-lactam variants of the classic Freidinger lactams[117] as conformationally restricted nucleators of β-turn structures. Starting from these scaffolds, specific cyclic RGD β-lactam peptidomimetics were also developed.[118]

Very recently, Galletti et al.[119] designed novel integrin ligands including a β-lactam scaffold, which can be regarded as an *N*-to-*C*β cyclic β^3-amino acid (Figure 17). The compounds **38** and **39** were readily prepared from the commercially available 4-acetoxy-azetidin-2-one. The carboxylic acid function at the C4 side chain of the β-lactam was introduction by Reformatsky reaction, followed by *N*-acylation to give the RGD mimetic **38**. The insertion of a further Gly at the C4 side chain afforded the longer compound **39**.

These new derivatives were tested in their ability to modulate the adhesion of integrin-expressing cells to immobilized FN. Surprisingly, the collected data support that the β-lactam derivatives present an interesting activity as αvβ3 and α5β1 integrin agonists. Indeed, **38** and **39** increased in a concentration-dependent manner the FN-mediated adhesion of K562 cells and SK-MEL-24 cells. In particular, ligand **38** exhibited higher affinity towards α5β1 integrin (EC_{50} = 1.2×10^{-8} M), while **39** was selective for integrin αvβ3 (EC_{50} = 1.1×10^{-8} M). Both ligands were unable (IC_{50} >1×10^{-4} M) to modify the adhesion of Jurkat E6.1 cells to vascular cell

adhesion molecule-1 (VCAM-1) mediated by α4β1 integrin, and the adhesion to intercellular adhesion molecule-1 (ICAM-1) mediated by αLβ2 integrin.

The new β-lactam derivatives maintained their ability to increase cell adhesion even in the absence of FN. In a second series of experiments, the wells of a standard test plate were coated by passive adsorption with either **38**, **39**, FN as a positive control, bovine serum albumin (BSA) as a negative control. K562 and SK-MEL-24 cells were seeded for adhesion; the two cell lines exhibited significant adhesion to both ligands, comparable to FN, while the cells did not adhere to wells coated with BSA. Antibodies of the β1 or αv integrin subunit added in advance to the cells blocked the adhesion mediated by **38** and **39**, strengthening the hypothesis that cell adhesion was mediated by the integrins αvβ3 and α5β1. Interestingly, the adhesion of K562 cells to both ligands was partially blocked by the selective αIIbβ3 integrin antagonist tirofiban. On the basis of these data, the authors conjectured that both α5β1 and αIIbβ3 integrins may contribute to mediate the adhesion of K562 cells induced by **38** and **39**.

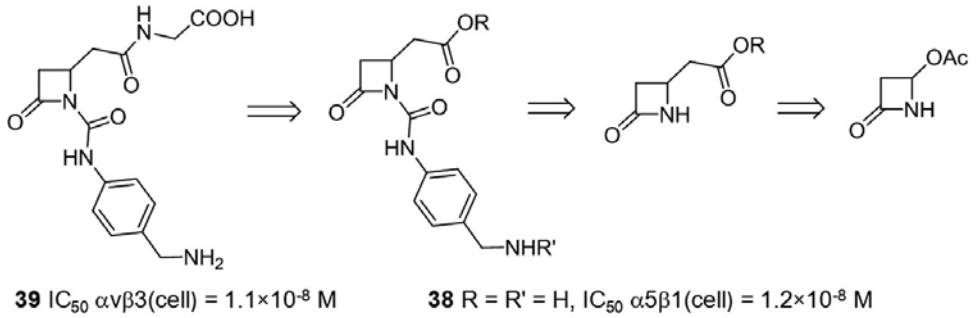

Figure 17 Retrosynthetic strategy for the *β*-lactam-containing RGD-like compounds **38** and **39**. IC50 values refer to integrin-expressing cells (cell).

5.2.2. Five-membered heterocyclic β-amino acidic cores

Dominguez et al. proposed a conformationally constrained *N*-aryl-γ-lactam scaffold to mimic the Arg-Gly dipeptide. This γ-lactam structurally resembled an *N*-to-Cα cyclic β^2-residue, and was obtained from nitroaniline and itaconic acid (Figure 18). The pure enantiomers of the γ-lactams were obtained via chemical resolution by means of the Evans' chiral auxiliary. When elaborated with various β-amino acids, the resulting ligands provided potent and selective αvβ3 antagonists. All compounds were assayed in competitive

electrochemiluminescent binding experiments using VN as specific αvβ3 receptor ligand, and FB for the αIIbβ3 receptor. The prototypic ligand **40** (IC_{50} = 0.7×10^{-9} M) is shown in Figure 18. Generally, the γ-lactam derivatives were highly selective for αvβ3 versus αIIbβ3.[120]

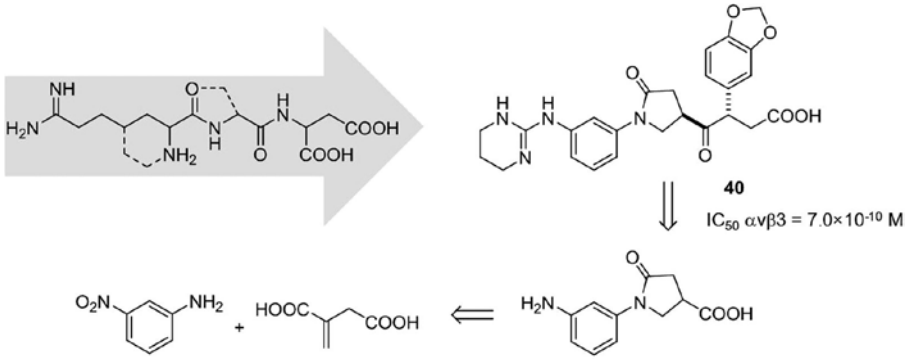

Figure 18 Rationale of the *N*-aryl-*γ* -lactam strategy and retrosynthesis of potent *αvβ*3 antagonist **40**. IC50 value refers isolated integrins.

Molecular-mechanics simulation indicated that the hindered rotation between the *ortho*-substituted central phenyl rings and the lactam imposes to the *N*-aryl-γ-lactam scaffold a well-defined conformation. Relative steric requirements provoke specific arrangements of the guanidine and carboxylate groups, hence influencing the degree of binding to αvβ3 integrin. Only the correct conformation of the central core allows the effective interaction with the receptor. The (*R*)-configuration of the γ-lactam was found to be essential for effective binding, as determined by the examination of the individual stereoisomers for other compounds of the series. The favored stereochemistry on the β-amino acid Asp mimic turned out to be the (*S*)-configuration, while chirality modification at the Asp mimic resulted in minor effects on the binding process.

In the last few years, the use of retro sequences of the classic RGD-binding motif for αvβ3 and α5β1-integrin has attracted significant attention.[40,71,99,101] By contrast, the retro strategy is still largely ignored for the design of ligands of the non RGD-binding α4β1 integrin. Gentilucci et al.[102] reported the first implementation of the retro-sequence strategy for the design of new analogues of the α4β1 integrin inhibitor MPUPA-Leu-Asp-Val-Pro-OH **41**, BIO1211,[121] where MPUPA is *o*-methylphenylurea phenylacetyl group (Figure 19). The retro sequences were composed of the β-amino acid (*S*)-pyrrolidine-3-carboxylic acid (or β^2-Pro) as a constrained core, Asp or *iso*Asp equipped with an aromatic cap at the *N*-terminus, and the amino variant 1-(4-

(aminomethyl)phenyl)-3-(*o*-methylphenyl)urea (AMPUMP) of the well-known α4-targeting MPUPA group.[102]

The structures of the novel peptidomimetics were designed on the basis of the models developed by 3D-QSAR analysis of large libraries of compounds containing diphenylureas. This approach led to the retro sequences BnCO-Asp-β[2]-Pro-AMPUMP **43**, and BnCO-*iso*Asp-β[2]-Pro-AMPUMP **44** (Figure 19B). As a variant, retro compounds incorporated an *N*-2,6-dicholorobenzoyl group instead of BnCO. BIO1211 **42** was chosen as α4β1 integrin antagonist reference compound, and the straight sequence MPUPA-β[2]-Pro-AspOBn **42** was examined for comparison purposes (Figure 19A).

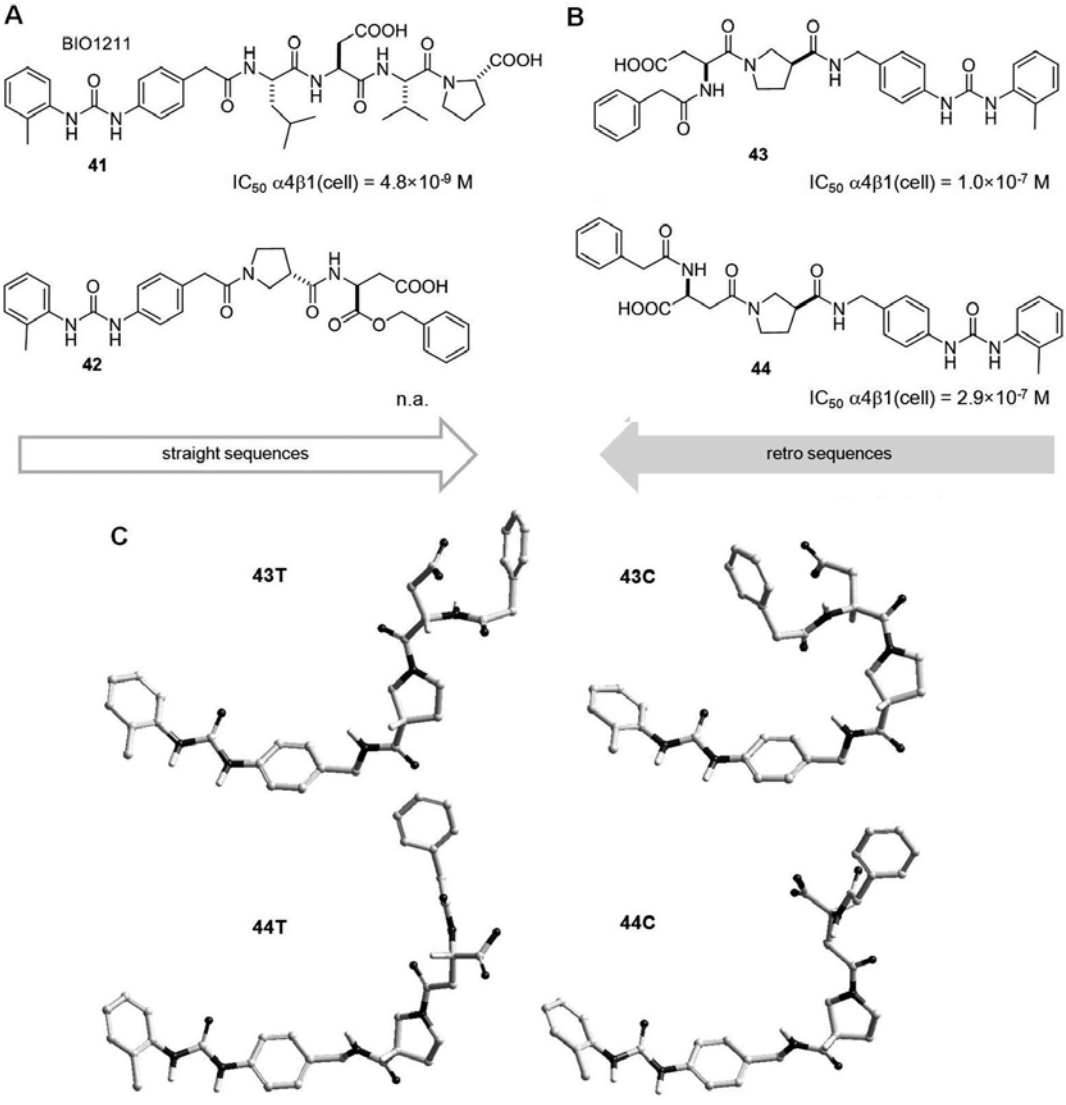

Figure 19 (**A**) Structures of BIO1211 **41** and the straight sequence containing *β*2-Pro **42**. (**B**) Structures of the retro sequences **43** and **44** containing *β*2-Pro. IC50 values refer to integrin-expressing cells (cell). (**C**) Representative low-energy structure for all-*trans*-**43T** and *trans-cis-trans*-**43C** (top), all-*trans*-**44T** and *trans-cistrans*-**44C** (bottom), consistent with ROESY analysis, and calculated by restrained MD.[102]

The binding of the peptidomimetics to α4β1 integrin was measured by Scintillation Proximity-binding Assay (SPA), using Jurkat cells consistently expressing human α4 integrin, and ^{125}I-FN as the specific radioligand. The straight sequence MPUMP- β^2-Pro-AspOBn **42** was not able to inhibit ^{125}I-FN binding. On the contrary, the retro compounds **43**, **44** caused concentration-dependent inhibition of ^{125}I-FN binding. The sequence BnCO-Asp-β^2-Pro-AMPUMP **43** showed IC_{50} of 1.0×10^{-7} M; the compound **44** containing *iso*Asp showed IC_{50} of 2.9×10^{-7} M. The analog of **43** equipped with the 2,6-dicholorobenzoyl group revealed modest micromolar affinity.

Subsequently, the ability of the new ligands to inhibit the adhesion of α4β1 integrin-expressing Jurkat cells to VCAM-1 was assayed. The reference compound **41** behaved as a potent α4β1 integrin ligand ($IC_{50} = 7.6\times10^{-9}$ M). Interestingly, the retro compounds **43** and **44** inhibited cell adhesion with an IC_{50} of 80 and 9.3×10^{-8} M, respectively, but did not show activity in cell adhesion assays aimed to evaluate potential antagonist activity toward αvβ3 integrin (SK-MEL-24 cells coated with VN). The peptidomimetic **42** and the 2,6-dicholorobenzoyl variants of **43** and **44** did not affect cell adhesion to a significant extent, confirming the results of the SPA assay discussed above

The significant biological activity of the structurally related **43** and **44** prompted the analysis of their preferred conformations by NMR spectroscopy in 8:2 DMSO-d_6/H_2O. Cryoprotective mixtures of high viscosity solvents, such as DMSO and water, have been utilized by several authors as excellent biomimetic media for NMR analysis.[122,123,124] As expected, the ^{1}H NMR spectra of both compounds revealed two sets of resonances, in about 1:1 ratio, corresponding to the *cis* and *trans* conformers of the peptide bond linking the pyrrolidine ring. Structures consistent with 2D ROESY were analyzed in a box of explicit water molecules by restrained molecular dynamics (MD); the representative geometries of all-*trans*-**43T**, *trans*-*cis*-*trans*-**43C**, all-*trans*-**44T**, *trans*-*cis*-*trans*-**44C**, are shown in Figure 19C.

Despite of the potential high flexibility of the linear ligands, the β-Pro scaffold induced markedly bent conformations. The most significant differences between the predominant conformations of **43** and **44** were found at the position of the aromatic group adjacent to Asp or *iso*Asp, respectively. This might be the consequence of the slightly different affinity values determined by SPA, confirming the relevant role of the flanking aromatic substituent for efficient binding of the receptor.

Apparently, the new compounds are less potent integrin antagonists compared with the reference BIO1211 **41**. However, the latter was previously found to be very unstable in heparinized blood, plasma and rat liver, lung and intestinal homogenates, being metabolized by hydrolytic cleavage of the terminal dipeptide moiety, giving a sequence much less active than the parent compound.[125,126] Because of their peptidomimetic nature, the sequences BnCO-Asp-β^2-Pro-urea **43** and BnCO-isoAsp-β^2-Pro-urea **44** were assumed to be significantly more stable, in particular upon consideration of the presence of the central β-Pro scaffold. The resistance to enzymatic degradation was estimated in mouse serum. After 120 min, **43** was degraded to a moderate extent (about 10%), and **44** was even more stable (<5% degradation) after incubation in the mouse serum. By contrast, BIO1211 **41** was almost completely hydrolyzed under the same conditions.

In this context, Tolomelli et al. employed isoxazolines as the central scaffolds of RGD peptidomimetics. These heterocyclic segments behave as flat, achiral β^2-proline analogues, which can be derivatized with substituents at the C5 of the pyrrolidine ring. Accordingly, the *trans*-5-hydroxyisoxazolidine-4-carboxylates of interest were prepared via the conjugate addition of hydroxyamine nucleophiles to alkylidene acetoacetates promoted by a Lewis-acid, and subsequent intra-hemiketalization.[127,128] For instance, racemic *trans*-5-hydroxyisoxazolidine-4-carboxylates were *N*-acylated with benzyl malonyl chloride; mesylation and base-induced elimination gave the corresponding racemic isoxazolines (Figure 20). The coupling of 4-nitrobenzylamine by conventional procedures and the reduction of the nitro group afforded the integrin ligands **45**. Further sequence elongation by introduction of a glycine gave the peptidomimetic **46**.[129]

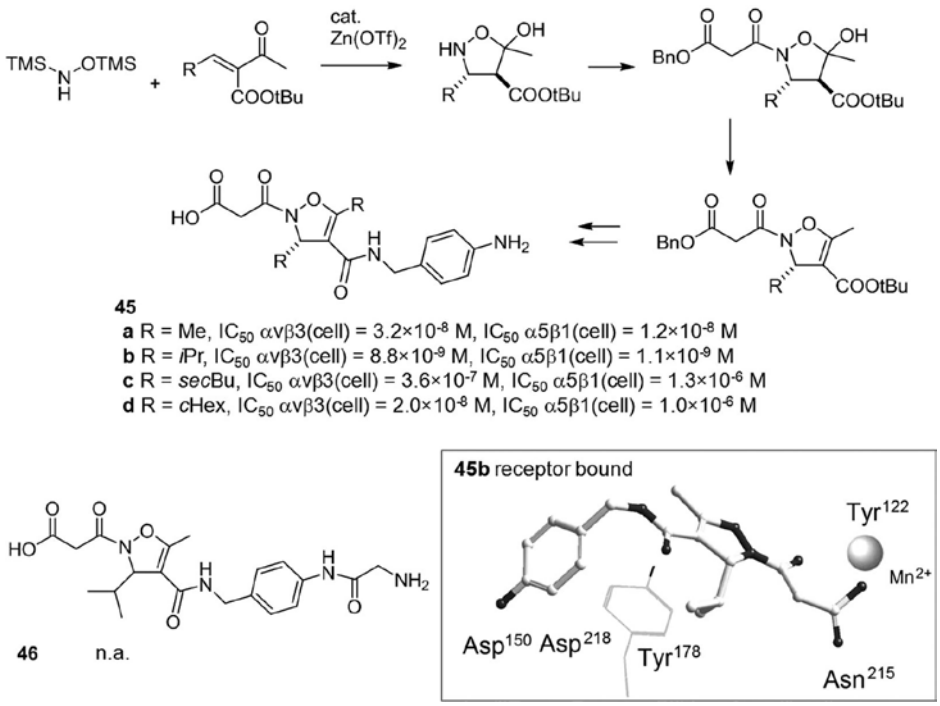

Figure 20 Relevant steps of the synthesis of RGD mimetics **45a-d** and **46** containing the flat isoxazoline core. IC50 values refer to integrin-expressing cells (cell). In the box: sketch of the docking (Glyde version 4.5) best pose of compound (*R*)-**45b** (thick lines) into the crystal structure45 of the extracellular domain of *αvβ3* integrin (the Mn2+ ion at MIDAS is rendered as a ball). Selected integrin residues involved in interactions with the ligand are highlighted; the stacking interaction between the heterocycle and Tyr178 (rendered in sticks) is also shown.

Experiments were performed to ascertain the ability of racemic compounds **45** and **46** to inhibit the adhesion of α5β1 integrin-expressing cells K562, or the adhesion of αvβ3 integrin-expressing cells SK-MEL-24, to immobilized FN. Among the various RGD mimetics tested, **45a** was an equally potent inhibitor of both αvβ3 and α5β1 integrin, with IC_{50} in the high nanomolar range; **45b** with R = *i*Pr exhibited the highest inhibitory activity against both αvβ3 and α5β1 integrins with of 8.8 and 1.1×10^{-9} M, respectively. The compound **45c** was poorly active towards both integrin types, while **45d** exhibited selectivity for αvβ3 integrins over α5β1. In contrast, the longer compound **46** was practically inactive. The effect of compound **45b** in integrin signaling *via* ERK was determined. Pre-incubation with **45b** significantly reduced the amount of ERK phosphorylation induced by FN in K562 cells.

A computational model for the binding of **45b** to αvβ3 integrin was built by automated docking computations. The ligand was docked into the 3D model of integrin αvβ3, as reported in the complex with cilengitide **3** (PDB ID: 1L5G).[45] Apart from the usual electrostatic interactions anticipated for RGD mimetics

including **3**, the computations highlighted a peculiar stacking effect between the 4-aminobenzylamine moiety of the ligand and the aromatic side chain of Tyr[178] of the αv subunit (Figure 20).

In the course of studies aimed at the development of in-peptide one-step ring closure to give peptidomimetics comprising rigid heterocyclic scaffolds, Gentilucci et al. obtained the 5-aminomethyloxazolidine-2,4-dione (Amo) scaffold.[130] The Amo ring was obtained in solution or in solid phase from isoserine (*iso*Ser) or other α-hydroxy-β-amino acids already present within the sequence of peptides, by treatment with disuccinimidyldicarbonate (DSC) and a catalytic amount of base (Figure 21A).

This Amo ring incorporated the α-hydroxy-β-amino acid and the amine function of the adjacent residue. This result was complementary to the previously observed reactions with sequences including β-hydroxy-α-amino acids, which gave under the same conditions oxazolidinone (Oxd)-peptides.[131,132] Indeed, depending on the stereochemistry, linear peptides including two consecutive β-hydroxy-α-amino acids gave rise to sequences Oxd-Oxd or ΔAbu-Oxd (ΔAbu, dehydroaminobutanoic acid). These scaffolds adopted well defined extended or folded conformations, in particular normal or inverse β-turns.[133]

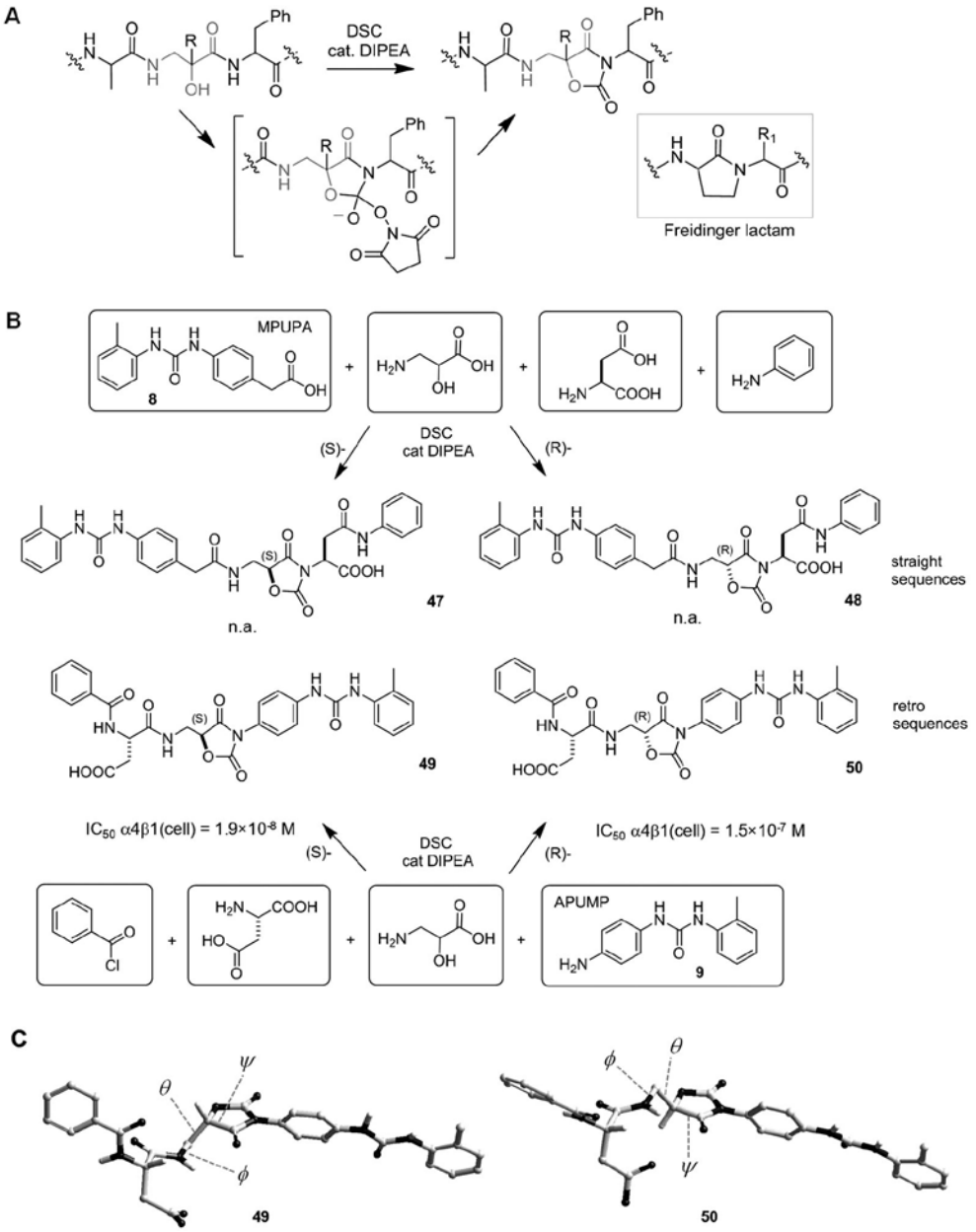

Figure 21 (**A**) The cyclization of linear peptides containing *α*-hydroxy-*β*-amino acids gave Amo dipeptide scaffolds. In the box: a classic Freidinger lactam. (**B**) Design of the straight Amo peptidomimetics MPUPAAmo-Asp(NHPh)-OH, (*S*,*S*)-**47** and (*R*,*S*)-**48**, and of the retro variants PhCOAsp(OH)-Amo-APUMP, (*S*,*S*)-**49** and (*S*,*R*)-**50**. IC50 values refer to integrin-expressing cells (cell). (**C**) Representative low-energy structures of **49** and **50** consistent with ROESY analysis and calculated by restrained MD in a box of standard TIP3P water molecules.

To date, the oxazolidine-2,4-dione heterocyclic core has found very little use in medicinal chemistry, the only notable example being a procedure for the synthesis of the 5-aminomethyl-3-oxazolidinone core of the antibiotic linezolid (LNZ) in enantiomerically pure form, *via* an Amo intermediate.[134] From the structural point of view, the Amo dipeptide represents an unprecedented β^2-homo analogue of the Freidinger lactam[117] (Figure 21A). The convenient synthetic procedure and the peculiar conformational features prompted to utilize the Amo α/β-dipeptide scaffold for the design and synthesis of mimetics of the well-known BIO1211 (**41**)[121] as

α4β1 integrin inhibitors.[135] The new peptidomimetics were readily prepared by connecting a diphenylurea pharmacophore and an aryl-substituted Asp, to (*S*)- or (*R*)-configured Amo scaffolds, obtained in turn by the expedient cyclization of the corresponding (*S*)- or (*R*)-i*so*Ser-containing sequences; different assemblies lead to "normal" (**47**, **48**) or retro-sequences (**49**, **50**) (Figure 21B). Only the retro sequences were able to inhibit the adhesion of the α4β1 integrin-expressing Jurkat cells to the ligand VCAM in a dose-dependent manner; in particular the homochiral **49** had IC_{50} in the 10^{-8} M range. Also, the two compounds showed remarkable chemical and enzymatic stability, as determined by incubation in mouse serum.

In the diastereoisomer **49**, the central dihedral angle θ (convention of Banerjee and Balaram[7]) of the Amo residue adopts a $+g$ conformation, consistent with the calculated geometries previously reported for β^2-amino acids. In the diastereoisomer **50** the PhCO-Asp group is positioned at the opposite side of the Amo ring with respect to **49**, and the central dihedral angle θ of Amo adopts a $-g$ conformation (due to the opposite stereochemistry, $-g$ and $+g$ of in (*R*)-Amo and (*S*)-Amo, respectively, correspond). In essence, the Amo scaffold of **49** imposes a preferential conformation, that is compatible with the 3D models (see Section 2) reported in the literature for BIO1211 **41** and similar compounds.

Very recently, BIO1211 **41** mimetics containing a dehydro-β-proline ring have been described.[136] The scaffolds present in these ligands were synthesized by means of a novel strategy, involving ring closing metathesis of a diallylamino derivative (Figure **22**).[137] Appendages to the central core were selected on the basis of literature precedent. The synthesized products were assayed for cell adhesion inhibition and in additional assays aimed to ascertain the effect of these purported α4β1 antagonists. A particular ligand, (*R*)-**51a,** was a good integrin ligand, showing $IC_{50} = 1.0\times10^{-8}$ M in the inhibition of α4β1 integrin-expressing Jurkat cells adhesion to VCAM-1. A strong dependence on the stereochemistry of the heterocyclic central core could be observed suggesting a preferred disposition of the lipophilic chain for (*R*) enantiomers. Modest activity was observed toward the homologous integrin α4β7, determined by the inhibition of RPMI8866 cells adhesion to the ECM ligand MadCam-1, while they did not display any activity toward α5β1, αLβ2, and αvβ3 integrins, analyzed using K-562 cells, Jurkat cells, SK-MEL-24 cells, and the ECM ligands FN, ICAM-1, and FN, respectively.

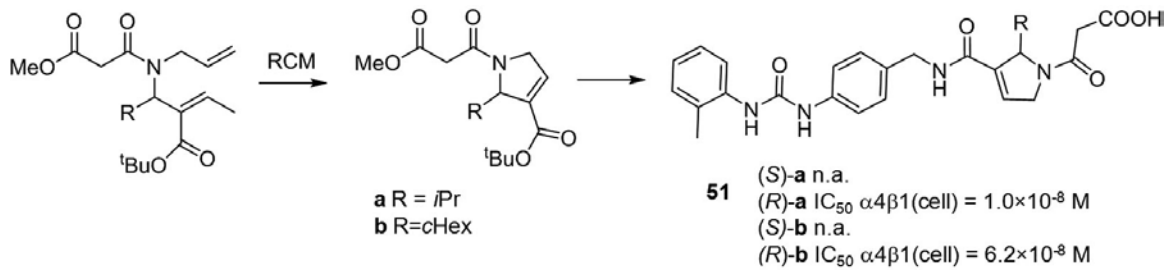

Figure 22 Synthesis of the dehydro-*β*-proline core, and elaboration of the *α*4*β*1 integrin ligands **51**. IC50 values refer to integrin-expressing cells (cell).

5.2.3. Six-membered β-amino acid-derived heterocyclic cores

Some years ago, Singh et al. developed and patented a 3D pharmacophore model of compounds presenting α4β1 inhibitory activity, which was utilized for the design of peptidomimetic ligands.[138] Among the most promising structures obtained *in silico*, a representative derivative is compound **52** containing the homo-β^2-proline (nipecotic acid) scaffold (Figure 23).

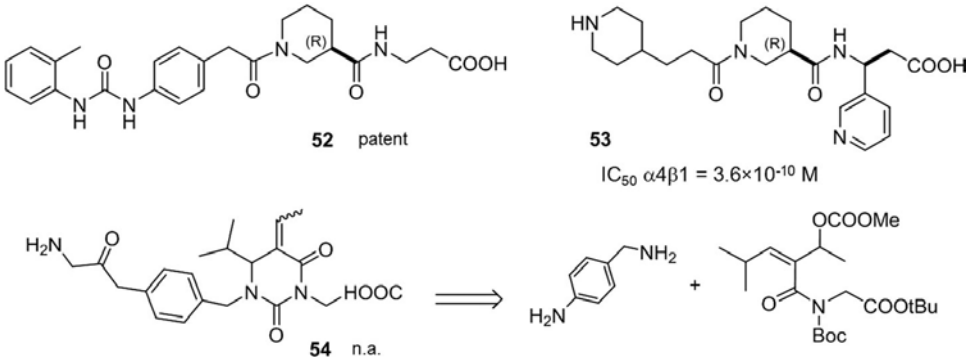

Figure 23 Integrin ligands 52–54 containing 6-membered heterocyclic scaffolds. IC50 value refers to isolate integrins.

The nipecotic acid scaffold is also present in the potent antiplatelet FB receptor (αIIbβ integrin) antagonist **53** developed by Hoekstra et al. (Figure 21). Indeed, the six-membered ring scaffold conferred the peptidomimetic ligand an IC_{50} value for α4β1/FB of 3.6×10^{-10} M, excellent *in vivo* stability, bioavailability, and adsorption. Oral administration (1 or 3 mg/kg in dogs) produced long-lasting (5-6 h) inhibition of platelet aggregation, but not in the reduction of platelet number.[139]

Finally, Tolomelli et al. synthesized the RGD mimetic **54** containing a dihydropyrimidine-2,4-dione scaffold, formally enclosing a 2-dehydro-$\beta^{2,3}$-aminoacid and a glycine residue.[113] This compound showed very

poor affinity (IC_{50} $>10^{-5}$ M) for integrins αvβ3 or α5β1 compared to the structurally related acyclic peptidomimetics.

6. Conclusions

In summary, in this review we present an overview of the state-of-the-art in the design and synthesis of peptidomimetic integrin ligands based on α/β-hybrid peptide structures. While α/β-peptides have been extensively investigated in the foldamer field, scarce attention has been paid so far to these small-molecules from the bioactivity point of view.[5] Generally, the integrin inhibitors described herein were readily assembled by connecting the pharmacophores to non-racemic β-residues, or to cyclic scaffolds of β-amino acid derivation, usually by expedient procedures.

The different assemblies presented here lead to a variety of 3D diverse structures, and some of the resulting compounds attained remarkable biological activity. The relatively variable receptor affinities were rationalized on the basis of the different 3D molecular geometries imposed by the scaffolds. This evidence supports the fact that the hybrid α/β-peptide approach can furnish bioactive peptidomimetics, potentially useful as diagnostic tools and as therapeutic agents for integrin-correlated diseases.

7. Acknowledgements

We thank CHIESI Foundation, Parma, Italia, for the unrestricted support to the present research (Project "*AsthmaZoè*: Nanostructured materials for the detection of markers of asthma and other correlated inflammatory diseases", 2015-2017); MIUR - PRIN 2010 (Project "Synthesis and biomedical applications of tumor-targeting peptidomimetics), for financial support; Francesca Gallo, Silvia Baldo, and Martina Vagnoni, for collaboration.

8. References

1. Gentilucci L, Tolomelli A, Squassabia F. Peptides and peptidomimetics in medicine, surgery and biotechnology. Curr Med Chem 2006;13:2449-2466.

2. Gentilucci L, De Marco, R Cerisoli L. Chemical modifications designed to improve peptide stability: Incorporation of non-natural amino acids, pseudo-peptide bonds, and cyclization. Curr Pharm Des 2010;16:3185-3203.

3. Liskamp RMJ, Rijkers DTS, Kruijtzer JAW, Kemmink J. Peptides and proteins as a continuing exciting source of inspiration for peptidomimetics. ChemBioChem 2011;12:1626-1653.

4. Juaristi E, Soloshonok V. Enantioselective Synthesis of β-Amino Acids. Second edition. New York:Wiley-VCH; 2005.

5. Cabrele C, Martinek TA, Reiser O, Berlicki L. Peptides containing β-amino acid patterns: challenges and successes in medicinal chemistry. J Med Chem 2014;57:9718-9739.

6. Lelais G, Seebach D. β^2-Amino acids - syntheses, occurrence in natural products, and as components of β-peptides. Biopolymers 2004;76:206-243.

7. Banerjee A, Balaram P. Stereochemistry of peptides and polypeptides containing omega amino acids. Curr Sci India 1997;73:1067-1077.

8. Vasudev PG, Chatterjee S, Shamala N, Balaram P. Structural chemistry of peptides containing backbone expanded amino acid residues: conformational features of β, γ, and hybrid peptides. Chem Rev 2011;111:657-687.

9. Horne WS, Gellman SH. Foldamers with heterogeneous backbones. Acc Chem Res 2008;41:1399-1408.

10. Seebach D, Gardiner J. β-Peptidic peptidomimetics. Acc Chem Res 2008;41:1366-1375.

11. Baldauf C, Günther R, Hofmann H.-J. Theoretical prediction of the basic helix types in α,β-hybrid peptides. Biopolymers 2006;84:408-413.

12. Guichard G, Huc I. Synthetic foldamers. Chem Commun 2011;47:5933-5941.

13. Martinek TA, Fülöp F. Peptidic foldamers: ramping up diversity. Chem Soc Rev 2012;41:687-702.

14. Kiss L, Fülöp F. Synthesis of carbocyclic and heterocyclic β-aminocarboxylic acids. Chem Rev 2014;114:1116-1169.

15. Goodman CM, Choi S, Shandler S, DeGrado WF. Foldamers as versatile frameworks for the design and evolution of function. Nat Chem Biol 2007;3:252-262.

16. Roy A, Prabhakaran P, Baruah PK, Sanjayan GJ. Diversifying the structural architecture of synthetic oligomers: the hetero foldamer approach. Chem Commun 2011;11593-11611.

17. Srichai MB, Zent R. Integrin structure and function. In: Zent R, Pozzi A. editors. Cell-extracellular matrix interactions in cancer. New York: Springer Science+Business Media, LLC; 2010. p19-41.

18 Pytela R, Pierschbacher MD, Ginsberg MH, Plow EF, Ruoslahti E. Platelet membrane glycoprotein IIb/IIIa: member of a family of Arg-Gly-Asp-specific adhesion receptors. Science 1986;231:1559-1562.

19. Desgrosellier JS, Cheresh DA. Integrins in cancer: biological implications and therapeutic opportunities. Nat Rev Cancer 2010;10:9-22.

20. Jackson DY. Alpha4 integrin antagonists Curr Pharm Des 2002;8:1229-1253.

21. Yang GX, Hagmann WK. VLA-4 antagonists: potent inhibitors of lymphocyte migration. Med Res Rev 2003;23:369-392

22. Perdih A, Dolenc MS. Small molecule antagonists of integrin receptors. Curr Med Chem 2010;17:2371-2392.

23. Cacciari B, Spalluto G. Non peptidic αvβ3 antagonists: recent developments. Curr Med Chem 2005;12:51-70.

24. Heckmann D, Kessler H. Design and chemical synthesis of integrin ligands. Methods Enzymol 2007;426:463-503.

25. Arosio D, Casagrande C; Manzoni L. Integrin-mediated drug delivery in cancer and cardiovascular diseases with peptide-functionalized nanoparticles. Curr Med Chem 2012;19:3128-3151.

26. Marelli UK, Rechenmacher F, Sobahi TR, Mas-Moruno C, Kessler H. Tumor targeting via integrin ligands. Front Oncol 2013;3:222,1-12.

27. Beer AJ, Kessler H, Wester HJ, Schwaiger M. PET imaging of integrin αvβ3 expression. Theranostics 2011;1:48-57.

28. Danhier F, Le Breton A, Préat V. RGD-based strategies to target αvβ3 integrin in cancer therapy and diagnosis. Mol Pharm 2012;9:2961-2973.

29. Gaertner FC, Kessler H, Wester HJ, Schwaiger M, Beer AJ. Radiolabelled RGD peptides for imaging and therapy. Eur J Nucl Med Mol Imaging. 2012;39:S126-138.

30. Meyer A, Auernheimer J, Modlinger A, Kessler H. Targeting RGD recognizing integrins: drug development, biomaterial research, tumor imaging and targeting. Curr Pharm Des 2006;12:2723-2647.

31. Newham P, Craig SE, Seddon GN, Schofield NR, Rees A, Edwards RM, Jones EY, Humphries MJ. α4 integrin binding interfaces on VCAM-1 and MAdCAM-1. Integrin binding footprints identify accessory binding sites that play a role in integrin specificity. J Biol Chem 1997;272:19429-19440.

32. Sheldrake HM, Patterson LH. Strategies to inhibit tumor associated integrin receptors: Rationale for dual and multi-antagonists. J Med Chem 2014;57:6301-6315.

33. Simon KO, Nutt EM, Abraham DG, Rodan GA, Duong LT. The αvβ3 integrin regulates α5β1-mediated cell migration toward fibronectin. J Biol Chem 1997;272:29380-29389.

34. Stachurska A, Elbanowski J, Kowalczyñska HM. Role of α5β1 and αvβ3 integrins in relation to adhesion and spreading dynamics of prostate cancer cells interacting with fibronectin under *in vitro* conditions. Cell Biol Int 2012;36, 883-892.

35. Christoforides C, Rainero E, Brown KK, Norman JC, Toker, A. PKD controls αvβ3 integrin recycling and tumor cell invasive migration through its substrate rabaptin-5. Dev Cell 2012;23:560-572.

36. Parvani JG, Galliher-Beckley AJ, Schiemann BJ, Schiemann WP. Targeted inactivation of β1 integrin induces β3 integrin switching that drives breast cancer metastasis by TGF-β. Mol Biol Cell 2013;24:3449-3459.

37. Haubner R, Gratias R, Diefenbach B, Goodman SL, Jonczyk A, Kessler H. Structural and functional aspects of RGD-containing cyclic pentapeptides as highly potent and selective integrin αvβ3 antagonists. J Am Chem Soc 1996;118:7461-7472

38. Henry C, Moitessier N, Chapleur, Y. Vitronectin receptor-αvβ3 integrin-antagonists: chemical and structural requirements for activity and selectivity. Mini Rev Med Chem 2002;2:531-542.

39. Pfaff M, Tangemann K, Müller B, Gurrath M, Müller G, Kessler H, Timpl R, Engel J. Selective recognition of cyclic RGD peptides of NMR defined conformation by αIIbβ3, αVβ3, and α5β1 integrins. J Biol Chem 1994;269:20233-20238.

40. Wermuth J, Goodman SL, Jonczyk A, Kessler H. Stereoisomerism and biological activity of the selective and superactive αvβ3 integrin inhibitor cyclo(-RGDfV-) and its retro-inverso peptide. J Am Chem Soc 1997;119:1328-1335.

41. Greco A, Maggini L, De Cola L, De Marco R, Gentilucci L. Diagnostic implementation of fast and selective integrin-mediated adhesion of cancer cells on functionalized Zeolite L monolayers. Bioconjug Chem 2015;26:1873-1878.

42. Dechantsreiter MA, Planker E, Mathä B, Lohof E, Hölzemann G, Jonczyk A, Goodman SL, Kessler H. N-Methylated cyclic RGD peptides as highly active and selective αvβ3 integrin antagonists. J Med Chem 1999;42:3033-3040.

43. Lohof E, Planker E, Mang C, Burkhart F, Dechantsreiter MA, Haubner R, Wester HJ, Schwaiger M, Hölzemann G, Goodman SL, Kessler H. Carbohydrate derivatives for use in drug design: Cyclic αv-selective RGD peptides. Angew Chem Int Edit 2000;39:2761-2764.

44. Stupp R, Hegi ME, Gorlia T, Erridge SC, Perry J, Hong YK, Aldape KD, Lhermitte B, Pietsch T, Grujicic D, Steinbach JP, Wick W, Tarnawski R, Nam DH, Hau P, Weyerbrock A, Taphoorn MJ, Shen CC, Rao N, Thurzo L, Herrlinger U, Gupta T, Kortmann RD, Adamska K, McBain C, Brandes AA, Tonn JC, Schnell O, Wiegel T, Kim CY, Nabors LB, Reardon DA, van den Bent MJ, Hicking C, Markivskyy A, Picard M, Weller M. Cilengitide combined with standard treatment for patients with newly diagnosed glioblastoma with methylated MGMT promoter (CENTRIC EORTC 26071-22072 study): a multicentre, randomised, open-label, phase 3 trial. Lancet Oncol 2014;15:1100-1108.

45. Xiong JP, Stehle T, Zhang R, Joachimiak A, Frech M, Goodman SL, Arnaout MA. Crystal structure of the extracellular segment of integrin αvβ3 in complex with an Arg-Gly-Asp ligand. Science 2002;296:151-155.

46. Marinelli L, Lavecchia A, Gottschalk KE, Novellino E, Kessler H. Docking studies on αvβ3 integrin ligands: pharmacophore refinement and implications for drug design. J Med Chem 2003;46:4393-4404.

47. Marinelli L, Meyer A, Heckmann D, Lavecchia A, Novellino E, Kessler H. Ligand binding analysis for human α5β1 integrin: strategies for designing new α5β1 integrin antagonists. J Med Chem 2005;48:4204-4207.

48. Heckmann D, Meyer A, Marinelli L, Zahn G, Stragies R, Kessler H. Probing integrin selectivity: rational design of highly active and selective ligands for the α5β1 and αvβ3 integrin receptor. Angew Chem Int Edit 2007;46:3571-3574.

49. Mould AP, Koper EJ, Byron A, Zahn G, Humphries MJ. Mapping the ligand-binding pocket of integrin α5β1 using a gain-of-function approach. Biochem J 2009;424:179-189.

50. Carlevaro CM, Da Silva JHM, Savino W, Caffarena ER. Plausible binding mode of the active α4β1 antagonist, Mk-0617, determined by docking and free energy calculations. J Theor Comput Chem 2013;12: 1-16.

51. You TJ, Maxwell DS, Kogan TP, Chen Q, Li J, Kassir J, Holland GW, Dixon RAF. A 3D structure model of integrin α4β1 complex: I. Construction of a homology model of β1 and ligand binding analysis Biophys J 2002;82:447-457.

52. Macchiarulo A, Costantino G, Meniconi M, Pleban K, Ecker G, Bellocchi D, Pellicciari R. Insights into phenylalanine derivatives recognition of VLA-4 integrin: from a pharmacophoric study to 3D-QSAR and molecular docking analyses. J Chem Inf Comput Sci 2004;44:1829-1839.

53. Thangapandian S, John S, Sakkiah S, Lee KW. Discovery of potential integrin VLA-4 antagonists using pharmacophore modeling, virtual screening and molecular docking studies. Chem Biol Drug Des 2011;78:289-300.

54. Springer TA, Zhu J, Xiao T. Structural basis for distinctive recognition of fibrinogen γC peptide by the platelet integrin αIIbβ3. Cell Biol. 2008;182:791-800.

55. Zhu J, Luo BH, Xiao T, Zhang C, Nishida N, Springer TA. Structure of a complete integrin ectodomain in a physiologic resting state and activation and deactivation by applied forces. Mol Cell. 2008;32:849-861.

56. Nagae M, Re S, Mihara E, Nogi T, Sugita Y, Takagi J. Crystal structure of α5β1 integrin ectodomain: atomic details of the fibronectin receptor. J Cell Biol. 2012;197:131-140.

57. Mas-Moruno C, Beck JG, Doedens L, Frank AO, Marinelli L, Cosconati S, Novellino E, Kessler H. Increasing αvβ3 selectivity of the anti-angiogenic drug cilengitide by *N*-methylation. Angew Chem Int Edit 2011;50:9496-9500.

58. Cupido T, Spengler J, Ruiz-Rodriguez J, Adan J, Mitjans F, Piulats J, Albericio F. Amide-to-ester substitution allows fine-tuning of the cyclopeptide conformational ensemble. Angew Chem Int Edit 2010;49:2732-2737.

59. Fernández-Llamazares AI, Adan J, Mitjans F, Spengler J, Albericio F. Tackling lipophilicity of peptide drugs: replacement of the backbone *N*-methyl group of cilengitide by *N*-oligoethylene glycol (N-OEG) chains. Bioconjug Chem. 2014;25:11-17.

60. Schuman F, Müller A, Koksch M, Müller G, Sewald N. Are *β*-amino acids *γ*-turn mimetics? Exploring a new design principle for bioactive cyclopeptides. J Am Chem Soc 2000;122:12009-12010.

61. Zimmermann D, Guthöhrlein EW, Malesević M, Sewald K, Wobbe L, Heggemann C, Sewald N. Integrin α5β1 ligands: biological evaluation and conformational analysis. ChemBioChem 2005;6:272-276.

62. Glenn MP, Kelso MJ, Tyndall JD, Fairlie DP. Conformationally homogeneous cyclic tetrapeptides: useful new three-dimensional scaffolds. J Am Chem Soc 2003;125:640-641.

63. Norgren AS, Büttner F, Prabpai S, Kongsaeree P, Arvidsson PI. β^2-Amino acids in the design of conformationally homogeneous cyclo-peptide scaffolds. J Org Chem 2006;71:6814-2681.

64. Gentilucci L, Cardillo G, Tolomelli A, Spampinato S, Sparta A, Squassabia F. Cyclotetrapeptide mimics based on a 13-membered, partially modified retro-inverso structure. Eur J Org Chem 2008;729-735.

65. Chorev M. The partial retro-inverso modification: A road traveled together. Biopolymers 2005;80:67-84.

66. Fletcher MD, Campbell MM. Partially modified retro-inverso peptides: Development, synthesis, and conformational behavior. Chem Rev 1998;98:763-795.

67. Gentilucci L, Cardillo G, Tolomelli A, Squassabia F, De Marco R, Chiriano G. Cyclopeptide analogs for generating new molecular and 3D diversity. Comb Chem High Throughput Screen 2009;12:929-939.

68. Dunitz JD, Waser J. Geometric constraints in six- and eight-membered rings J Am Chem Soc 1972;94:5645-5650.

69. Kessler H, Gratias R, Hessler G, Gurrath M, Müller G. Conformation of cyclic peptides. Principle concepts and the design of selectivity and superactivity in bioactive sequences by 'spatial screening'. Pure & Appl Chem 1996;68:1201-1205.

70. Gentilucci L, Cardillo G, Tolomelli A, De Marco R, Garelli A, Spampinato S, Spartà A, Juaristi E. Synthesis and conformational analysis of cyclotetrapeptide mimetic β-turn templates and validation as 3D scaffolds. ChemMedChem 2009;4:517-523.

71. Gentilucci L, Cardillo G, Spampinato S, Tolomelli A, Squassabia F, De Marco R, Bedini A, Baiula M, Belvisi L, Civera M. Antiangiogenic effect of dual/selective α5β1/αvβ3 integrin antagonists designed on partially modified retro-inverso cyclotetrapeptide mimetics. J Med Chem 2010;53:106-118.

72. Urman S, Gaus K, Yang Y, Strijowski U, Sewald N, De Pol S, Reiser O. The constrained amino acid β-Acc confers potency and selectivity to integrin ligands. Angew Chem Int Edit 2007;46:3976-3978.

73. Royo M, Van Den Nest W, del Fresno M, Frieden A, Yahalom D, Rosenblatt M, Chorev M, Albericio F. Solid-phase syntheses of constrained RGD scaffolds and their binding to the αvβ3 integrin receptor. Tetrahedron Lett 2001;42:7387-7391.

74. da Ressurreição ASM, Vidu A, Civera M, Belvisi L, Potenza D, Manzoni L, Ongeri S, Gennari, C Piarulli U. Cyclic RGD-peptidomimetics containing bifunctional diketopiperazine scaffolds as new potent integrin ligands. Chem Eur J 2009;15:12184-12188.

75. Marchini M, Mingozzi M, Colombo R, Guzzetti I, Belvisi L, Vasile F, Potenza D, Piarulli U, Arosio D, Gennari C. Cyclic RGD peptidomimetics containing bifunctional diketopiperazine scaffolds as new potent integrin ligands. Chem Eur J 2012;18:6195-6207.

76. Guzzetti I, Civera M, Vasile F, Araldi EM, Belvisi L, Gennari C, Potenza D, Fanelli R, Piarulli U. Determination of the binding epitope of RGD peptidomimetics to αvβ3 and αIIbβ3 integrin-rich intact cells by NMR and computational studies. Org Biomol Chem 2013;11:3886-3893.

77. Mayer M, Meyer B. Characterization of ligand binding by saturation transfer difference NMR spectroscopy. Angew Chem Int Edit 1999;38:1784-1788.

78. Colombo R, Mingozzi M, Belvisi L, Arosio D, Piarulli U, Carenini N, Perego P, Zaffaroni N, De Cesare M, Castiglioni V, Scanziani E, Gennari C. Synthesis and biological evaluation (*in vitro* and *in vivo*) of cyclic arginine-glycine-aspartate (RGD) peptidomimetic-paclitaxel conjugates targeting integrin αvβ3. J Med Chem 2012;55:10460-10474.

79. Scarborough RM. Structure-activity relationships of β-amino acid-containing integrin antagonists. Curr Med Chem 1999;6:971-981.

80. Gentilucci L, Cardillo G, Squassabia F, Tolomelli A, Spampinato S, Sparta A, Baiula M. Inhibition of cancer cell adhesion by heterochiral Pro-containing RGD mimetics. Bioorg Med Chem Lett. 2007;17:2329-2333.

81. Krysko AA, Chugunov BM, Malovichko OL, Andronati SA, Kabanova TA, Karaseva TL, Kiriyak AV. Novel fibrinogen receptor antagonists. RGDF mimetics, derivatives of 4-(isoindoline-5-yl)amino-4-oxobutyric acid. Bioorg Med Chem Lett 2004;14:5533-5535.

82. Goodman SL, Hölzemann G, Sulyok GA, Kessler H. Nanomolar small molecule inhibitors for αvβ6, αvβ5, and αvβ3 integrins. J Med Chem. 2002;45:1045-1051.

83. Malovichko OL, Petrus AS, Krysko AA, Kabanova TA, Andronati SA, Karaseva TL, Kiriyak AV. Derivatives of 7-amino-1,2,3,4-tetrahydroisoquinoline and isophthalic acids as novel fibrinogen receptor antagonists. Bioorg Med Chem Lett 2006;16:5294-5297.

84. Krysko AA, Krysko OL, Kabanova TA, Andronati SA, Kabanov VM. Derivatives of tetrahydroisoquinoline: synthesis and initial evaluation of novel non-peptide antagonists of the αIIbβ3-integrin. Bioorg Med Chem Lett. 2010;20:4444-4446.

85. Zablocki, JA, Rico JG, Garland RB, Rogers TE, Williams K, Schretzman LA, Rao SA, Bovy PR, Tjoeng FS, Lindmark RJ, Toth M, Zupec M, McMackins DE, Adams SP, Miyano M, Markos CS, Milton MN, Paulson S, Herin M, Jacquin P, Nicholson N, Panzer-Knodle SG, Haas NF, Page JD, Szalony JA, Taite BB, Salyers AK, King LW, Campion J. Feigen LP. Potent in vitro and in vivo inhibitors of platelet aggregation based upon the Arg-Gly-Asp sequence of fibrinogen. (Aminobenzamidino)succinyl (ABAS) series of orally active fibrinogen receptor antagonists. J Med Chem 1995;38:2378-2394.

86. Batt DG, Petraitis JJ, Houghton GC, Modi DP, Cain GA, Corjay MH, Mousa SA, Bouchard PJ, Forsythe MS, Harlow PP, Barbera FA, Spitz SM, Wexler RR, Jadhav PK. Disubstituted indazoles as potent antagonists of the integrin αvβ3. J Med Chem 2000;43:41-58.

87. Smallheer JM, Weigelt CA, Woerner FJ, Wells JS, Daneker WF, Mousa SA, Wexler RR, Jadhav PK. Synthesis and biological evaluation of nonpeptide integrin antagonists containing spirocyclic scaffolds. Bioorg Med Chem Lett 2004;14:383-387.

88. Feuston BP, Culberson JC, Duggan ME, Hartman GD, Leu CT, Rodan SB. Binding model for nonpeptide antagonists of αvβ3 integrin. J Med Chem 2002;45:5640-5648.

89. Li F, Jas GS, Qin G, Li K, Li Z. Synthesis and evaluation of bivalent, peptidomimetic antagonists of the αvβ3 integrins. Bioorg Med Chem Lett 2010;20:6577-6580.

90. Shin IS, Jang BS, Danthi SN, Xie J, Yu S, Le N, Maeng JS, Hwang IS, Li KC, Carrasquillo JA, Paik CH. Use of antibody as carrier of oligomers of peptidomimetic αvβ3 antagonist to target tumor-induced neovasculature. Bioconjug Chem 2007;18:821-828.

91. Hood JD, Bednarski M, Frausto R, Guccione S, Reisfeld RA, Xiang R, Cheresh DA. Tumor regression by targeted gene delivery to the neovasculature. Science 2002;296:2404-2407.

92. Neubauer S, Rechenmacher F, Beer AJ, Curnis F, Pohle K, D'Alessandria C, Wester HJ, Reuning U, Corti A, Schwaiger M, Kessler H. Selective imaging of the angiogenic relevant integrins α5β1 and αvβ3. Angew Chem Int Edit 2013;52:11656-11659.

93. Klim JR, Fowler AJ, Courtney AH, Wrighton PJ, Sheridan RT, Wong ML, Kiessling LL. Small-molecule-modified surfaces engage cells through the αvβ3 integrin. ACS Chem Biol 2012;7:518-525.

94. Curnis F, Longhi R, Crippa L, Cattaneo A, Donossola E, Bachi E, Corti A. Spontaneous formation of L-isoaspartate and gain of function in fibronectin. J Biol Chem 2006;281:36466-36476.

95. Takahashi V, Leiss M, Moser M, Ohashi T, Kitao T, Heckmann D, Pfeifer A, Kessler H, Takagi J, Erickson HP, Fässler R. The RGD motif in fibronectin is essential for development but dispensable for fibril assembly, J Cell Biol 2007;178:167-178.

96. Xu J, Maurer LM, Hoffmann BR, Annis DS, Mosher DF. *iso*-DGR sequences do not mediate binding of fibronectin *N*-terminal modules to adherent fibronectin-null fibroblasts. J Biol Chem 2010;285:8563-8571.

97. Spitaleri A, Ghitti M, Mari S. Alberici L, Traversari C, Rizzardi GP, Musco G. Use of metadynamics in the design of *iso*DGR-based αvβ3 antagonists to fine-tune the conformational ensemble. Angew Chem Int Edit 2011;50:1832-1836.

98. Ghitti M, Spitaleri A, Valentinis B, Mari S, Asperti C, Traversari C, Rizzardi GP, Musco G. Molecular dynamics reveal that *iso*DGR-containing cyclopeptides are true αvβ3 antagonists unable to promote integrin allostery and activation. Angew Chem Int Edit 2012;51:7702-7705.

99. Frank AO, Otto E, Mas-Moruno C, Schiller HB, Marinelli L, Cosconati S, Bochen A, Vossmeyer D, Zahn G, Stragies R, Novellino E, Kessler H. Conformational control of integrin-subtype selectivity in *iso*DGR peptide motifs: a biological switch. Angew Chem Int Edit 2010;49: 9278-9281.

100. Bochen A, Marelli UK, Otto E, Pallarola D, Mas-Moruno C, Di Leva FS, Boehm H, Spatz JP, Novellino E, Kessler H, Marinelli L. Biselectivity of isoDGR peptides for fibronectin binding integrin subtypes α5β1 and αvβ6: conformational control through flanking amino acids, J Med Chem 2013;56:1509-1519.

101. Mingozzi M, Dal Corso A, Marchini M, Guzzetti I, Civera M, Piarulli U, Arosio D, Belvisi L, Potenza D, Pignataro L, Gennari C. Cyclic *iso*DGR peptidomimetics as low-nanomolar αvβ3 integrin ligands. Chem Eur J 2013;19:3563-3567.

102. Dattoli SD, De Marco R, Baiula M, Spampinato S, Greco A, Tolomelli A, Gentilucci L. Synthesis and assay of retro-α4β1 integrin-targeting motifs. Eur J Med Chem 2014;73:225-232.

103. Osterkamp F, Wehlan H, Koert U, Wiesner M, Raddatz P, Goodman SL. Synthesis and biological evaluation of dianhydrohexitol integrin antagonists. Tetrahedron 1999;55:10713-10734.

104. Corbett JW, Graciani NR, Mousa SA, DeGrado WF. Solid-phase synthesis of a nonpeptide RGD mimetic library: new selective alphavbeta3 integrin antagonists. Bioorg Med Chem Lett 1997;7.1371-1376.

105. Lohof E, Planker E, Mang C, Burkhart F, Dechantsreiter MA, Haubner R, Wester HJ, Schwaiger M, Holzemann G, Goodman SL, Kessler H. Carbohydrate derivatives for use in drug design: cyclic αv-selective RGD peptides. Angew Chem Int Edit 2000;39:2761-2764.

106. Moitessier N, Dufour S, Chrétien F, Thiery J-P, Maigret B, Chapleur Y. Design, synthesis and preliminary biological evaluation of a focused combinatorial library of stereodiverse carbohydrate-scaffold-based peptidomimetics. Bioorg Med Chem 2001;9.511-523.

107. Kantlehner M, Finsinger D, Meyer J, Schaffner P, Jonczyk A, Diefenbach B, Nies B, Kessler H. Selective RGD-mediated adhesion of osteoblasts at surfaces of implants. Angew Chem Int Edit 1999;38:560-562.

108. Hayashi Y, Katada J, Harada T, Tachiki A, Iijima K, Takiguchi Y, Muramatsu M, Miyazaki H, Asari T, Okazaki T, Sato Y, Yasuda E, Yano M, Uno I, Ojima I. GPIIb/IIIa integrin antagonists with the new conformational restriction unit, trisubstituted β-amino acid derivatives, and a substituted benzamidine structure. J Med Chem 1998;41:2345-2360.

109. Cardillo G, Gennari A, Gentilucci L, Mosconi E, Tolomelli A, Troisi S. Synthesis of chiral non-racemic intermediates and Arg-Gly-Asp mimetics by CaLB-catalyzed resolution. Tetr Asymm 2010;21:96-102.

110. Unpublished results.

111. Benfatti F, Cardillo G, Gentilucci L, Mosconi E, Tolomelli A. Synthesis of dehydro-β-amino esters via highly regioselective amination of allylic carbonates. Org Lett 2008;10:2425-2428.

112. Cardillo G, Gennari A, Gentilucci L, Mosconi E, Tolomelli A, Troisi S. Dehydro-β-amino acid containing peptides as promising sequences for drug development. Eur J Org Chem 2009;5991-5997.

113. Tolomelli A, Baiula M, Belvisi L, Viola A, Gentilucci L, Troisi S, Dattoli SD, Spampinato S, Civera M, Juaristi E, Escudero M. Modulation of αvβ3- and α5β1-integrin-mediated adhesion by dehydro-β-amino acid containing peptidomimetics. Eur J Med Chem 2013;66:258-268.

114. Zhu J, Zhu J, Negri A, Provasi D, Filizola M, Coller BS, Springer TA. Closed headpiece of integrin αIIbβ3 and its complex with an αIIbβ3-specific antagonist that does not induce opening Blood 2010;116:5050-5059.

115. Unpublished results.

116. Hruby VJ, Balse PM. Conformational and topographical considerations in designing agonist peptidomimetics from peptide leads. Curr Med Chem 2000;7:945-970.

117. Freidinger RM, Veber DF, Perlow DS, Brooks JR, Saperstein R. Bioactive conformation of luteinizing hormone-releasing hormone: evidence from a conformationally constrained analog. Science 1980;210:656-658.

118. Aizpurua JM, Ganboa JI, Palomo C, Loinaz I, Oyarbide J, Fernandez X, Balentová E, Fratila RM, Jiménez A, Miranda JI, Laso A, Avila S, Castrillo JL. Cyclic RGD β-lactam peptidomimetics induce differential gene expression in human endothelial cells. ChemBioChem. **2011**, *12*, 401-405.

119. Galletti P, Soldati R, Pori M, Durso M, Tolomelli A, Gentilucci L, Dattoli S.D, Baiula M, Spampinato S, Giacomini D. Targeting integrins αvβ3 and α5β1 with new β-lactam derivatives. Eur J Med Chem 2014;18:284-293.

120. Xi N, Arvedson S, Eisenberg S, Han N, Handley M, Huang L, Huang Q, Kiselyov A, Liu Q, Lu Y, Nunez G, Osslund T, Powers D, Tasker AS, Wang L, Xiang T, Xu S, Zhang J, Zhu J, Kendall R, Dominguez C. *N*-Aryl-γ-lactams as integrin αvβ3 antagonists. Bioorg Med Chem Lett 2004;14:2905-2909.

121. Lin Kc, Ateeq HS, Hsiung SH, Chong LT, Zimmerman CN, Castro A, Lee WC, Hammond CE, Kalkunte S, Chen LL, Pepinsky RB, Leone DR, Sprague AG, Abraham WM, Gill A, Lobb RR, Adams SP. Selective, tight-binding inhibitors of integrin α4β1 that inhibit allergic airway responses. J Med Chem 1999;42:920-934.

122. Temussi PA, Picone D, Saviano G, Amodeo P, Motta A, Tancredi T, Salvadori S, Tomatis R. Conformational analysis of an opioid peptide in solvent media that mimic cytoplasm viscosity. Biopolymers 1992;32:367-372.

123. Borics A, Töth G. Structural comparison of mu-opioid receptor selective peptides confirmed four parameters of bioactivity. J Mol Graph Modell 2010;28:495-505.

124. Sikorska E, Slusarz MJ, Lammek B. Conformational studies of vasopressin analogues modified with N-methylphenylalanine enantiomers in dimethyl sulfoxide solution. Biopolymers 2006;82:603-614.

125. Karanam BV, Jayra A, Rabe M, Wang Z, Keohane C, Strauss J, Vincent S. Effect of enalapril on the *in vitro* and *in vivo* peptidyl cleavage of a potent VLA-4 antagonist. Xenobiotica 2007;37:487-502.

126. Fisher AL, DePuy E, Jayaraj A, Raab C, Braun M, Ellis-Hutchings M, Zhang J, Rogers JD, Musson DG. LC/MS/MS plasma assay for the peptidomimetic VLA4 antagonist I and its major active metabolite II: for treatment of asthma by inhalation. J Pharm Biomed Anal 2002; 27:57-71.

127. Benfatti F, Cardillo G, Gentilucci L, Mosconi E, Tolomelli A, Lewis acid induced highly regioselective synthesis of a new class of substituted isoxazolidines. Synlett 2008;2605-2608.

128. Benfatti F, Cardillo G, Contaldi S, Gentilucci L, Mosconi E, Tolomelli A, Juaristi E, Reyes-Rangel G. A convenient synthesis of functionalized isoxazolines and related 5-hydroxyisoxazolidine-4-carboxylates.Tetrahedron 2009;65: 2478-2483.

129. Tolomelli A, Gentilucci L, Mosconi E, Viola A, Dattoli SD, Baiula M, Spampinato S, Belvisi L, Civera M. Development of isoxazoline-containing peptidomimetics as dual αvβ3 and α5β1 integrin ligands. Chem Med Chem 2011;6:2264-2272.

130. Greco A, Tani S, De Marco R, Gentilucci L. Synthesis and analysis of the conformational preferences of 5-aminomethyloxazolidine-2,4-dione scaffolds: first examples of β^2- and $\beta^{2,2}$-homo-Freidinger lactam analogues. Chem Eur J 2014;20:13390-13404.

131. Gentilucci L, Tolomelli A, De Marco R, Tomasini C, Feddersen S. Synthesis of constrained peptidomimetics containing 2-oxo-1,3-oxazolidine-4-carboxylic acids. Eur J Org Chem 2011;4925-4930.

132. De Marco R, Tolomelli A, Campitiello M, Rubini P, Gentilucci L. Expedient synthesis of pseudo-Pro-containing peptides: towards constrained peptidomimetics and foldamers. Org Biomol Chem 2012;10:2307-2317.

133. De Marco R, Greco A, Rupiani S, Tolomelli A, Tomasini C, Pieraccini S, Gentilucci L. In-peptide synthesis of di-oxazolidinone and dehydroamino acid-oxazolidinone motifs as β-turn inducers. Org Biomol Chem 2013;11:4273-4420.

134. Greco A, De Marco R, Tani S, Giacomini D, Galletti P, Tolomelli A, Juaristi E, Gentilucci L. Convenient synthesis of the antibiotic linezolid via an oxazolidine-2,4-dione intermediate derived from the chiral building block isoserine. Eur J Org Chem 2014;7614-7620.

135. De Marco R, Dattoli SD, Baiula M, Spampinato S, Greco A, Gentilucci L. 5-Aminomethyloxazolidin-2,4-dione hybrid α/β-dipeptide scaffolds as inductors of constrained conformations: applications to the synthesis of integrin antagonists. Biopolymers 2015;104:636-649.

136. Tolomelli A, Baiula M, Viola A, Ferrazzano L, Gentilucci L, Dattoli SD, Spampinato S, Juaristi E, Escudero M. Dehydro-β-proline containing peptidomimetics as selective α4β1 integrin antagonists: a stereochemical recognition in ligand-receptor interaction. ACS Med Chem Lett **2015**; 701-706.

137. Tolomelli A, Gentilucci L, Mosconi E, Viola A, Paradisi E. A straightforward route to enantiopure 2-substituted-3,4-dehydro-β-proline via ring closing metathesis. Amino Acids 2011:575-586.

138. Singh J, Zheng Z, Sprague P, Van Vlijmen H, Castro AC, Adams SP. Molecular model for VLA-4 inhibitors, and inhibitor identification. PCT Int. Appl. (1998), WO 9804913 A119980205.

139. Hoekstra WJ, Maryanoff BE, Damiano BP, Andrade-Gordon P, Cohen JH, Costanzo MJ, Haertlein BJ, Hecker LR, Hulshizer BL, Kauffman JA, Keane P, McComsey DF, Mitchell JA, Scott L, Shah RD, Yabut SC. Potent, orally active GPIIb/IIIa antagonists containing a nipecotic acid subunit. Structure-activity studies leading to the discovery of RWJ-53308. J Med Chem 1999;42:5254-5265.

Figure captions

Figure 1. Structures of α-, β^2-, β^3-, and $\beta^{2,3}$-amino acids (following Seebach's nomenclature[6]); the grey arrow shows the extra torsional angle θ (convention of Banerjee and Balaram[7]).

Figure 2. A The RGD and LDVP minimal binding motifs. **B** Structure and extended conformation in solution of **1**. **C** Structure and kinked conformation in solution of **2**. IC_{50} values refer to isolated integrins. The 3D structures were determined by two-dimensional NMR in combination with restrained and free molecular dynamics simulations.[37]

Figure 3 Structure c[RGDf-*N*(Me)V], cilengitide **3**; in the box: sketch of the main interactions of **3** with the αvβ3 binding site, as determined from the crystal structure of the complex (PDB ID: 1L5G); the ball represents a Mn^{+2} ion.[45] Di-*N*-methylated **4**, depsi-analogue of cilengitide **5**, and *N*-oligoethylene glycol substituted analogue **6**. IC_{50} values refer to isolated integrins or to integrin-expressing cells (cell).

Figure 4. Cyclopentapeptides **7** and **8**. In the box: the cyclotetrapeptide αvβ3 antagonist **9**, rationally designed by incorporation of a β-amino acid as a *pseudo* γ-turn inducer; the RGD sequence forms a complementary γ-turn; 3D structure of **9** determined by 2D NMR, distance geometry, and restrained molecular dynamics simulations.[60] Cyclohexapeptide α5β1 antagonist **10**. IC_{50} values refer to isolated integrins or to integrin-expressing cells (cell).

Figure 5. A Structure and backbone conformation of c[β-Phe-ψ(NHCO)Ala-ψ(NHCO)Gly-Phe] **11**.[64] **B** Structure and conformation of c[(*S*)-β^2-Phe-D-Pro-Lys-Phe] **12**.[63] Conformations determined by 2D NMR and molecular dynamics; some side chains have been omitted for clarity. **C** Structures of PR-CTP RGD mimetics **13**, **14**. IC_{50} values refer to integrin-expressing cells (cell).

Figure 6. Schematic Dunitz-Waser topographic depiction of the eight PR-CTP models (enantiomeric pairs), showing the *S*/*R* stereochemistry of the Cα, and the distances (Å) between the Cβ atoms. Grey arrows indicate the *pseudo*-axial or *pseudo*-equatorial disposition of the side chains (Cα-Cβ vectors).

Figure 7. Structures of the PR-CTP RGD mimetics **15** and **16**; IC_{50} values refer to isolated integrins or to integrin-expressing cells (cell). **A**,**B** The α5β1/αvβ3 mixed integrin antagonist **15** inhibits bFGF-induced formation of capillary-like tubes of HUVEC on Matrigel; **A** HUVEC plated on Matrigel in the presence of

bFGF; **B** HUVEC treated with compound **15** (1 μM), black bar = 100 μm. **C** Mean numbers of tubes per square millimeter ± SEM; * P<0.01, ** P < 0.05 vs control (Newman-Keuls test after ANOVA). **D** Overlap of the backbone structures of **15** (black) and **16** (grey), determined by ROESY and molecular dynamics.[71]

Figure 8. Sketches of the structures of **15** and **16**[71] determined by molecular docking (Glyde version 4.5) of the ligands within the crystal structure of the integrin αvβ3 (PDB ID: 1L5G).[45]

Figure 9 A Bioactive conformation of the αvβ3-selective c[RGDf(*N*-Me)V], cilengitide **3**, showing the distances (Å) between the pharmacophores (grey digits and grey dashed lines) and between Cβ atoms of Asp, D-Phe, and Arg (black digits and black dashed lines). **B** Dunitz-Waser sketch of **3**. **C** Dunitz-Waser sketches of (*S*,*R*,*S*)-CTP (top), and (*S*,*S*,*S*)-CTP (bottom), models of **15** and **16**, respectively.

Figure 10. Structures of the (+)- and (-)-β-Acc, and β-Acc-containing peptides **17** and **18.** Lowest-energy conformations obtained by restrained MD calculations based on experimental C-C bond distance information. IC_{50} values refer to integrin-expressing cells (cell).

Figure 11. In the box: structures of cyclic RGD-peptidomimetics **19** and **20** containing diketopiperazine scaffolds, and 3D structure of **20** as obtained by restrained Monte Carlo/Stochastic Dynamics (MC/SD) simulations based on experimental bond distance information, showing a pseudo β-turn at DKP-Arg. Diastereomers **21A** and **21B**, resulting from hindered rotation. Structure of the c[DKP-RGD]-paclitaxel conjugate **22**. IC_{50} values refer to isolated integrins.

Figure 12. Structure of an integrin antagonist-conjugated MoAb **23**, of a lipid-conjugated integrin antagonist **24**, and of a NODAGA-conjugated integrin antagonist **25**.

Figure 13. Structures of cyclic pentapeptides **26**, **27** containing the *iso*DGR motif, and of the cyclic *iso*DGR peptidomimetics **28** and **29** containing the bifunctional DKP scaffolds; 3D molecular structure of **26**, **27**,[99,100] and *trans*-(3*S*,6*R*)-DKP-*iso*DGR **29**[101] obtained by restrained MC/SD simulations based on experimental bond distance information, followed by energy minimization. IC_{50} values refer to isolated integrins.

Figure 14. Structures of the αIIbβ3 integrin antagonists **30** and **31** containing the trisubstituted β-residues; in the box: retrosynthesis of the β-residues.

Figure 15. General strategies for obtaining sequences **32**, **33** containing enantiopure β-amino acids, including the RGD mimetic **34**, by CaLB-catalyzed resolution of racemic β-amino acid derivatives. IC_{50} value refers to integrin-expressing cells (cell).

Figure 16. A Synthesis of enantiomerically pure allylic carbonates and synthesis of dehydro-β-amino esters through amination of allylic carbonates. **B** In the box: ligands **35-37** containing dehydro-β-amino acid scaffolds, examined for integrins αvβ3 and/or α5β1. IC_{50} values refer to integrin-expressing cells (cell).

Figure 17. Retrosynthetic strategy for the β-lactam-containing RGD-like compounds **38** and **39**. IC_{50} values refer to integrin-expressing cells (cell).

Figure 18. Rationale of the *N*-aryl-γ-lactam strategy and retrosynthesis of potent αvβ3 antagonist **40**. IC_{50} value refers isolated integrins.

Figure 19. A Structures of BIO1211 **41** and of the straight sequence containing β^2-Pro **42**. **B** Structures of the retro sequences **43** and **44** containing β^2-Pro. IC_{50} values refer to integrin-expressing cells (cell). **C** Representative low-energy structure for all-*trans*-**43T** and *trans*-*cis*-*trans*-**43C** (top), all-*trans*-**44T** and *trans*-*cis*-*trans*-**44C** (bottom), consistent with ROESY analysis, and calculated by restrained MD.[102]

Figure 20. Relevant steps of the synthesis of RGD mimetics **45a-d** and **46** containing the flat isoxazoline core. IC_{50} values refer to integrin-expressing cells (cell). In the box: sketch of the docking (Glyde version 4.5) best pose of compound (*R*)-**45b** (thick lines) into the crystal structure[45] of the extracellular domain of αvβ3 integrin (the Mn^{2+} ion at MIDAS is rendered as a ball). Selected integrin residues involved in interactions with the ligand are highlighted; the stacking interaction between the heterocycle and Tyr^{178} (rendered in sticks) is also shown.

Figure 21. A The cyclization of linear peptides containing α-hydroxy-β-amino acids gave Amo dipeptide scaffolds. In the box: a classic Freidinger lactam. **B** Design of the straight Amo peptidomimetics MPUPA-Amo-Asp(NHPh)-OH, (*S*,*S*)-**47** and (*R*,*S*)-**48**, and of the retro variants PhCOAsp(OH)-Amo-APUMP, (*S*,*S*)-**49** and (*S*,*R*)-**50**. IC_{50} values refer to integrin-expressing cells (cell). **C** Representative low-energy structures of **49** and **50** consistent with ROESY analysis and calculated by restrained MD in a box of standard TIP3P water molecules.

Figure 22. Synthesis of the dehydro-β-proline core, and elaboration of the α4β1 integrin ligands **51**. IC_{50} values refer to integrin-expressing cells (cell).

Figure 23. Integrin ligands **52-54** containing 6-membered heterocyclic scaffolds. IC_{50} value refers to isolate integrins.

Biosketches

Rossella De Marco, obtained her *laurea* in Chimistry and Pharmaceutical Sciences (CTF) at the University of Bologna in 2005, and the Ph. D. in Chemical Sciences in 2011 (Synthesis of Modified Amino Acids and Insertion in Peptides and Mimetics. Structural Aspects and Impact on Biological Activity). In 2013 she entered the Young Investigator Programme, Fondazione Umberto Veronesi. Presently, she is interested in the development of new methods for the synthesis of peptidomimetics.

Alessandra Tolomelli graduated in Chemistry in 1994 and received her Ph.D. degree in Chemistry in 1998 at the University of Bologna, working under the supervision of Prof. G. Cardillo. During the Ph.D. she spent a period at the University of California Santa Cruz, working in the group of Prof. J. Konopelsky. She is currently research associate at the University of Bologna. Her research interest mainly focus on beta-amino acids and in their introduction into bioactive peptidomimetics and in their conjugation with diagnostics and cytotoxics.

Eusebio Juaristi was born in Querétaro (México) in 1950 and studied Chemistry at Instituto Tecnológico de Monterrey (B. Sc.) and at the University of North Carolina in Chapel Hill (Ph. D.). Following postdoctoral stays in the University of California-Berkeley and Syntex, California, he returned to Mexico in 1979, to the Chemistry Department of CINVESTAV-IPN, where he is currently Emeritus Professor of Chemistry. He has been Visiting Professor at the ETH-Zurich (1985-1986 and 1992-1993), UC-Berkeley (1999-2000) and RWTH-Aachen (2013). In 1998 he received Mexico's Presidential Medal of Science and in 2006 he became a member of El Colegio Nacional, highest academic distinction in Mexico.

Luca Gentilucci is Associate Professor in organic and bioorganic chemistry at the University of Bologna. He graduate in Chemistry with a thesis on the chemistry of nitrones, and received his Ph. D. with Prof. Cardillo presenting a thesis on the use of heterocyclic intermediates for the synthesis of non-natural amino acids. He expanded the study of azirines and aziridines in Nijmegen with Prof. Binne Zwanemburg. He went back to Bologna as Research Associate for the Interdept. Biotechnology Research Centre, then he returned to the Dept. of Chemistry "G. Ciamician" as Associate Professor. Presently, his main research interests are in the field of the bioactive peptidomimetics (antibiotics, opioids, integrin inhibitors. etc).